CALIFORNIA
ENERGY COMMISSION

Energy Research and Development Division

FINAL PROJECT REPORT

Performance-Based Earthquake Engineering Assessment Tool for Natural Gas Storage and Pipeline Systems

Task C – Seismic Response of Wells and Caprocks

Gavin Newsom, Governor
July 2022

PREPARED BY:

Primary Authors:
Jonny Rutqvist, Tsubasa Sasaki, Keurfon Luu, Preston Jordan, Yingqi Zhang, William Foxall

Energy Geosciences Division
Lawrence Berkeley National Laboratory
1 Cyclotron Road, Berkeley, CA 94563
510-486-5432
https://eesa.lbl.gov/

Jennie Watson-Lamprey, Micaela Largent, Barry Zheng

Slate Geotechnical Consultants
2927 Newbury St Suite A, Berkeley, CA 94703
510-277-3325
https://slategeotech.com/

Contract Number: PIR-18-003

PREPARED FOR:
California Energy Commission

Yahui Yang
Project Manager

Laurie ten Hope
Deputy Director
ENERGY RESEARCH AND DEVELOPMENT DIVISION

Drew Bohan
Executive Director

ACKNOWLEDGEMENTS

The authors thank California Energy Commission for funding this project, the project partners Pacific Earthquake Engineering Research Center (PEER), UC Berkeley, UC San Diego, University of Nevada Reno, the NHERI SimCenter at UC Berkeley, and subcontractors Lettis Consultants International (LCI) and Thomas O'Rourke, as well as the Technical Advisory Committee for providing project guidance.

This research study was funded by the California Energy Commission, under Contract No. PIR 18-003. The opinions, findings, conclusions, and recommendations expressed in this publication are those of the authors and do not necessarily reflect the view of California Energy Commission and its employees, the State of California, the Pacific Earthquake Engineering Research (PEER) Center, and the Regents of the University of California.

PREFACE

The California Energy Commission's (CEC) Energy Research and Development Division manages the Natural Gas Research and Development Program, which supports energy-related research, development, and demonstration not adequately provided by competitive and regulated markets. These natural gas research investments spur innovation in energy efficiency, renewable energy and advanced clean generation, energy-related environmental protection, energy transmission and distribution and transportation.

The Energy Research and Development Division conducts this public interest natural gas-related energy research by partnering with RD&D entities, including individuals, businesses, utilities and public and private research institutions. This program promotes greater natural gas reliability, lower costs and increases safety for Californians and is focused in these areas:

- Buildings End-Use Energy Efficiency.
- Industrial, Agriculture and Water Efficiency
- Renewable Energy and Advanced Generation
- Natural Gas Infrastructure Safety and Integrity.
- Energy-Related Environmental Research
- Natural Gas-Related Transportation.

Task C: Final Report – Seismic Response of Wells and Caprocks is an interim report for the Performance-Based Earthquake Engineering Assessment Tool for Natural Gas Storage and Pipeline Systems project (PIR-18-003) conducted by the Lawrence Berkeley National Laboratory, Berkeley. The information from this project contributes to the Energy Research and Development Division's Natural Gas Research and Development Program.

For more information about the Energy Research and Development Division, please visit the CEC's research website (www.energy.ca.gov/research/) or contact the CEC at 916-327-1551.

ABSTRACT

This report is one of a series of reports documenting the methods and findings of a multi-year, multi-disciplinary project conducted by the Pacific Earthquake Engineering Research Center (PEER) with the Lawrence Berkeley National Laboratory (LBNL) and funded by the California Energy Commission (CEC). The overall project is titled "*Performance-based Earthquake Engineering Assessment Tool for Natural Gas Storage and Pipeline Systems*" henceforth referred to as the "*OpenSRA* Project."

The overall goal of the *OpenSRA* project is to create an open-source research-based seismic risk assessment tool for natural gas infrastructure that can be used by utility stakeholders to better understand state-wide risks, prioritize mitigation, plan new gas infrastructure, and help focus post-earthquake repair work.

The project team includes researchers from LBNL, UC Berkeley, UC San Diego, University of Nevada Reno, the NHERI SimCenter at UC Berkeley, and Slate Geotechnical Consultants and its subcontractors Lettis Consultants International (LCI) and Thomas O'Rourke. Focused research to advance the seismic risk assessment tool was conducted by Task Groups, each addressing a particular area of study and expertise, and collaborating with the other Task Groups.

This report is the product of Task Group C: Seismic Response of Wells and Caprocks and it summarizes targeted research related to seismic impact on underground gas storage facilities, and integrity of wells and caprocks. The work is divided into the main tasks of (1) direct fault shear across wells, (2) ground motion (shaking) impact on wells, and (3) potential caprock leakage along activated faults. In each of these three tasks, advanced full-physics modeling was performed for sensitivity and fragility analyses with the goal of providing usable input to the development of fragility (probability of failure) curves in *OpenSRA*. Relevant damage measures were selected as (1) plastic strain in casing and tubing during direct fault shear across wells, (2) maximum bending moment for ground motion impact on wells, and (3) cumulative gas leakage amount for potential caprock (fault) leakage. The variability of these damage measures for a given fault shear displacement or for a given seismic shaking intensity was evaluated by varying model parameters over relevant uncertainty ranges. The method and steps demonstrated in this report could subsequently be followed by consideration of additional scenarios or more site-specific information to improve the fragility functions developed for the *OpenSRA* seismic risk assessment tool.

Keywords: Underground gas storage, wells, faults, caprock, seismic, ground motion, fault activation, strain, gas leakage

Please use the following citation for this report:

Rutqvist, Jonny; Tsubasa Sasaki; Keurfon Luu; Preston Jordan; Yingqi Zhang; William Foxall, Jennie Watson-Lamprey, Micaela Largent, Barry Zheng, 2022. *Performance-Based Earthquake Engineering Assessment Tool for Natural Gas Storage and Pipeline Systems, Task C Final Report - Seismic Response of Wells and Caprocks.* California Energy Commission.

TABLE OF CONTENTS

Page

LIST OF FIGURES

Page

LIST OF TABLES

EXECUTIVE SUMMARY

Introduction

This report is one of a series of reports documenting the methods and findings of a multi-year, multi-disciplinary project conducted by the Pacific Earthquake Engineering Research Center (PEER) with the Lawrence Berkeley National Laboratory (LBNL) and funded by the California Energy Commission (CEC). The overall project is titled "*Performance-based Earthquake Engineering Assessment Tool for Natural Gas Storage and Pipeline Systems*" henceforth referred to as the "*OpenSRA* Project."

The overall goal of the *OpenSRA* project is to create an open-source research-based seismic risk assessment tool for natural gas infrastructure that can be used by utility stakeholders to better understand state-wide risks, prioritize mitigation, plan new gas infrastructure, and help focus post-earthquake repair work.

The project team includes researchers from LBNL, UC Berkeley, UC San Diego, University of Nevada Reno, the NHERI SimCenter at UC Berkeley, and Slate Geotechnical Consultants and its subcontractors Lettis Consultants International (LCI) and Thomas O'Rourke of Cornell University. Focused research to advance the seismic risk assessment tool was conducted by Task Groups, each addressing a particular area of study and expertise, and collaborating with the other Task Groups.

This report is the product of the Task Group C: Seismic Response of Wells and Caprocks. The report presents targeted research to advance *OpenSRA*, focusing on the integrity and vulnerability of wells and caprocks associated with underground gas storage (UGS) facilities. Large uncertainties and challenges exist when assessing the impact of seismic ground motion (shaking) and direct fault shear displacements on UGS facilities, as such events are rare. This means that there are very limited field data from which to derive empirical relations for predicting damage from future events. The research presented in this report is aimed at reducing the uncertainties associated with assessing the impact of seismic events on California UGS facilities and providing usable input to the *OpenSRA* software.

Project Purpose

The purpose of the work carried out under Task C is to perform targeted research on the impact of seismic ground motion (shaking) and direct fault shear displacements on UGS facilities. The advanced full-physics numerical modeling employed in this research can to some extent overcome the challenges resulting from the lack of empirical data and reduce the uncertainties in assessing the potential seismic impacts on UGS facilities. The objective of the research is to develop and apply full-physics modeling that includes parameter sensitivity analyses to provide usable input for the development of fragility (probability of failure) functions to *OpenSRA*.

Project Approach

The challenges in assessing the seismic impact on underground storage facilities were approached top-down, starting with an historic assessment from published literature, a review of relevant characteristics of California UGS facilities and wells and an assessment of potential changes in fault permeability caused by fault displacement. These provide the basis for the full-physics numerical modeling. Numerical sensitivity studies were first performed to determine the most significant parameters for assessing the impact of; (1) direct fault shear across wells, (2) seismic ground motion (shaking) impact on wells, and (3) potential caprock leakage along an activated fault.

In the case of direct fault shear across wells, the approach was to derive the relationship between fault shear displacement and strain in vital well components, whereas for ground shaking impact on wells the maximum bending moments from prescribed ground motions were evaluated. These analyses were conducted for typical California UGS well designs as identified from public records.

The assessment of potential caprock leakage along an activated fault is perhaps the most challenging task. This task requires an assessment of how a fault might dilate and transmit fluids after being activated. This requires an estimate of the volume of gas that could leak out through the dilated fault. The approach was taken to provide a conservative worst-case scenario of the potential opening of the fault assuming a high fault fluid transmissivity and to estimate the potential gas leakage for such a scenario. As the probability of dilation and gas leakage is so small, the conservatism is not expected to significantly influence the overall risk assessment.

Another challenge encountered in the project is the high computational demands for some of the full-physics model simulations. In the case of dynamic ground motion simulations, high computational demands led to the selection of a relatively simple, manageable numerical simulation approach. The LBNL research team working on the full-physics modeling took advantage of internal expertise on California gas storage facilities and data, and frequent interactions with LCI on fault characteristics, external experts in the Technical Advisory Committee (TAC) on gas well technology, and with Slate Geotechnical Consultants on the inputs and data needed for the development of fragility functions.

Project Results

An assessment and review of published historic data indicated that in terms of seismic impact on USG caprocks and well integrity, permanent shear displacement of a fault intersecting the gas storage overburden and reservoir could be expected to pose the highest risk, while seismic ground shaking is likely to damage only the shallowest part of a well. Four dominant California USG well configurations in terms of cementing and casing designs were identified from public records and used for the analysis.

Sensitivity analyses of the impact of direct fault shear displacement across wells showed that fault geometry parameters, such as fault angle relative to the well and fault width, are the most significant parameters to model to approximate the fragility curves for all types of well configurations. Cement properties were also found to be significant if the segment of the well that is displaced is cemented. The modeling further showed that uncemented well segments can resist greater fault displacement than cemented segments, with respect to both casing and tubing damage. The detailed well geometry, including the diameters of casing and tubing, also has a significant influence on the well response to a fault displacement.

Sensitivity analyses of the impact of ground shaking on UGS wells showed that the maximum bending moment in wells is mainly affected by a set of three parameters, namely the height and mass of the wellhead and soil strength. The dynamic ground motion modeling further showed that the resulting maximum bending moment depends on the dimensions of the well and the peak input ground motion, which in the present simulations is peak ground acceleration, and that the maximum bending moment occurs only a few meters below the ground surface. The results of the sensitivity analysis of bending moment caused by seismic loading utilized more than a thousand parameter cases.

The sensitivity analysis of the impact of fault shear across a gas storage reservoir caprock showed that gas leakage would not occur when the gas storage pressure is well below the hydrostatic water pressure. In the case of a gas storage pressure above hydrostatic pressure, the leakage rates were calculated for the worst-case scenario of a fault substantially dilated by shear activation. Changes in fault fluid transmissivity is an important parameter that was assumed to be dependent on the fault shear displacement according to empirical scaling relations with fault width and rupture length. Other parameters affecting the gas leakage rate are geometric and hydraulic factors, such as the thickness of the caprock and the permeabilities of the gas reservoir and overlying rock units.

The three subtasks to assess the impact of direct fault shear across wells, seismic ground shaking, and potential caprock leakage along an activated fault have provided results that will be used for deriving fragility functions to be used in *OpenSRA*. The method and steps demonstrated in this report could subsequently be followed by consideration of additional scenarios and/or more site-specific information to further improve the fragility functions used in the *OpenSRA* seismic risk assessment tool.

CHAPTER 1: Introduction

This report is one of a series of reports documenting the methods and findings of a multi-year, multi-disciplinary project conducted by the Pacific Earthquake Engineering Research Center (PEER) with the Lawrence Berkeley National Laboratory (LBNL) and funded by the California Energy Commission (CEC). The overall project is titled "*Performance-based Earthquake Engineering Assessment Tool for Natural Gas Storage and Pipeline Systems*" henceforth referred to as the "*OpenSRA* Project."

The overall goal of the *OpenSRA* project is to create an open-source research-based seismic risk assessment tool for natural gas infrastructure that can be used by utility stakeholders to better understand state-wide risks, prioritize mitigation, plan new gas infrastructure, and help focus post-earthquake repair work.

The probabilistic seismic risk tool developed in this project follows the widely accepted risk methodology pioneered by Cornell (1968). A seismic source characterization is used to develop a suite of earthquake scenarios with associated rates of occurrence to represent the seismic hazard. Fault ruptures and the resulting ground deformation are generated for each earthquake scenario to represent the seismic loading, which includes a map of ground motion parameters. This scenario-based seismic parameter map is overlaid on the infrastructure system, and the seismic loading is related to the capacities of the infrastructure to calculate the seismic performance of the natural gas system for the scenario. By repeating the process for all the scenarios in the suite, the tool can evaluate the seismic risk to the system.

A user-driven research approach was used to develop *OpenSRA* to be used easily by regulators and utilities, and to include updated models and methods for the seismic demands and capacities that control the seismic risk for natural gas systems. The project includes several innovative approaches that improve the basic methodology and distinguish this project's approach from standard approaches currently used. Current risk studies developed by the utilities use risk scoring approaches that are highly subjective and qualitative. They do not incorporate properly the uncertainties in the seismic demand and in the fragility of the system and its components. Targeted research was conducted in this project to improve the characterization of uncertainty of key inputs to the seismic risk assessment tool. The seismic risk methodology employed in this project provides quantitative estimates of the probabilistic seismic risk. For risk-informed decision-making processes, the reliability of the risk estimates needs to be considered because this can be significant, particularly for large, rare earthquakes.

The project team includes researchers from LBNL, UC Berkeley, UC San Diego, the University of Nevada, Reno, the NHERI SimCenter at UC Berkeley, and Slate Geotechnical Consultants and its subcontractors Lettis Consultants International (LCI) and Thomas O'Rourke. Focused research to advance the seismic risk assessment tool was conducted by Task Groups, each addressing a particular area of study and expertise, and collaborating with the other Task Groups. The Task Groups are:

- Task A: Fault Displacement

- Task B: Liquefaction-induced deformation and seismically induced slope displacement
- Task C: Performance of natural gas storage well casings and caprock
- Task D: Performance of gas storage and pipeline system surface infrastructure
- Task E: Smart gas infrastructure sensing of wells and pipeline connections performance
- Task F: Synthesis of component fragilities into a system performance model

This report is the product of Task Group C: Performance of natural gas storage well casings and caprock. The report summarizes targeted research aimed at quantifying and reducing the uncertainties associated with the assessment of the impacts of seismic events on underground gas storage facilities, including impacts on caprock and wells for both ground shaking and direct fault shear displacement. This research includes an historic assessment of published data and a review of California UGS facilities and wells, followed by advanced full-physics numerical modeling. As an illustrative example, Figure 1 shows a cross section through a gas storage facility and a hypothetical fault activation that results in a shearing impact on a well. In this example, some damage and straining of the well assembly have occurred but the well may still be operational without any gas leakage.

Figure 1: A Well Deformed by Fault Displacement

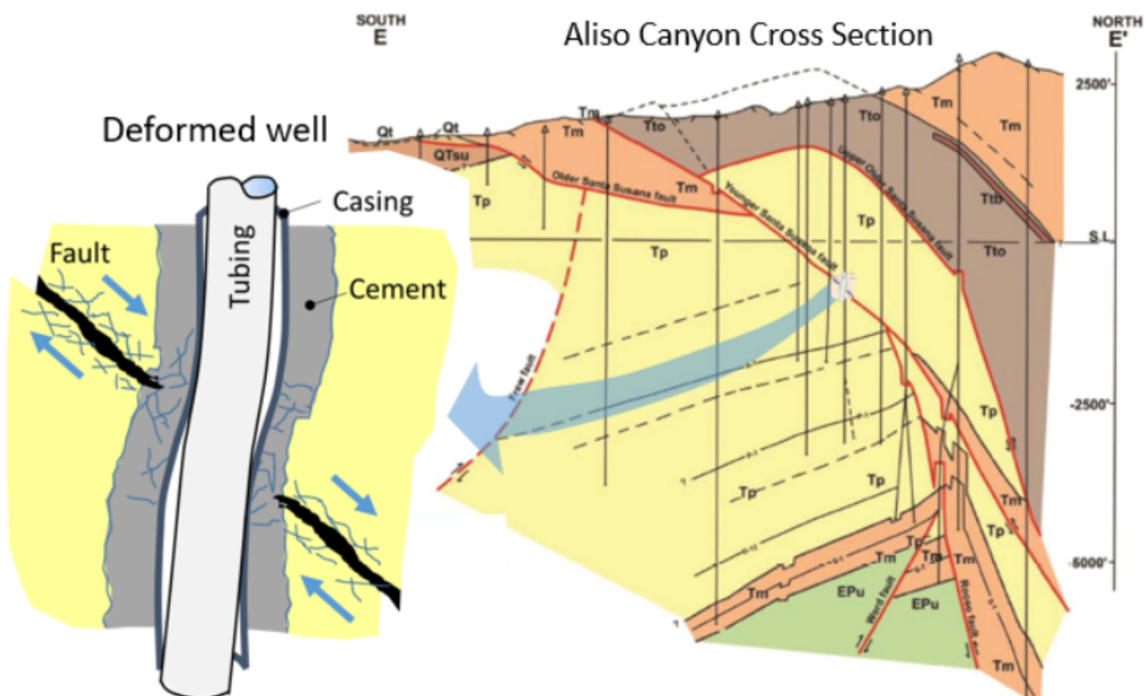

The figure shows a schematic of a well that is damaged by shear along an existing fault but may still be functioning (left). Vertical cross section through Aliso Canyon Gas Storage facility showing vertical wells intersecting faults (right).

Source: Left figure Lawrence Berkeley National Laboratory (2022); right figure Davis et al., (2015)

Full-physics modeling was conducted to simulate such straining of well components as a result of direct fault shear displacement. Similar full-physics modeling was performed to assess ground motion (shaking) impact on wells and potential caprock leakage along an activated fault. The results from the model simulations were then used to develop fragility (probability of failure) functions for the *OpenSRA*. Full technical details for the research performed under Task Group C are available in three comprehensive technical reports written by the LBNL team (Sasaki et al., 2022; Luu et al., 2022; Zhang et al., 2022).

CHAPTER 2: Project Approach

The challenges in assessing the seismic impact on underground storage facilities was approached top-down, starting from an historic impact assessment from published literature, a review of relevant characteristics of California underground gas storage facilities and gas storage wells, an assessment of potential changes in fault permeability caused by fault displacement, followed by the advanced full-physics numerical modeling. The research was divided into the three modeling subtasks summarized schematically in Figure 2:

1. direct fault shear across wells,
2. ground motion (shaking) impact on wells, and
3. potential caprock gas leakage.

In each of the three subtasks, advanced full-physics modeling was performed for sensitivity and fragility analysis with the goal of providing input that can be used to develop fragility curves, shown in Figure 2, for the *OpenSRA* tool. The research team from LBNL working on the full-physics modeling took advantage of internal LBNL expertise on California gas storage facilities and data, and frequent interactions with LCI on fault characteristics, external experts in the TAC on gas well technology, and with Slate Geotechnical Consultants on inputs and data needed for the development of fragility functions.

Figure 2: Fragility Curve Development for USG Subsurface Integrity

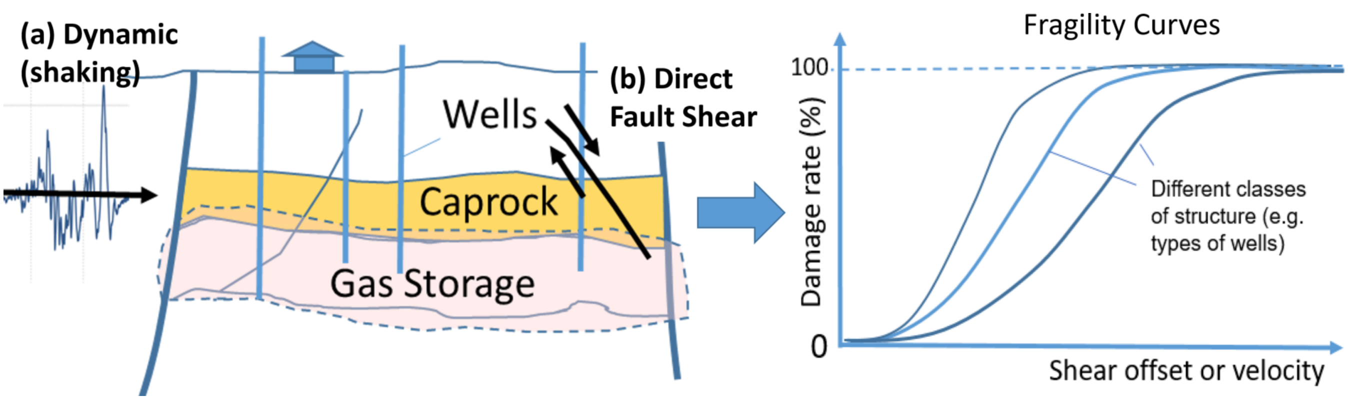

A schematic of impact of dynamic (shaking) impact and direct fault shear impact on a hypothetical underground gas storage facility (left) that are modeled for input for the development of fragility curve (right).

Source: Lawrence Berkeley National Laboratory (2022)

Historic Assessment

There are no well documented cases of subsurface seismic damage to underground gas storage facilities in the United States, or perhaps anywhere else. In a compilation of underground gas storage events around the world, Evans (2009) concluded that most incidents related to gas storage at depleted oil/gas reservoirs involved gas leaks and explosions. A more recent review focusing on California gas storage facilities is provided in a report for the California Council on Science and Technology (CCST, 2018), which in turn referred to the reviews by Evans (2009), Evans and Schultz (2017), and Folga et al. (2016).

In CCST (2018) California incidents are extracted out of Evans and Schultz (2017) and it is concluded that well-related leakage has been by far the most common failure mode for loss of containment incidents in California UGS facilities. In contrast, compilations of UGS failures worldwide suggest that loss of containment incidents at UGS facilities worldwide are four times more likely to involve above-ground infrastructure (valves, pipes, wellheads, compressors, and other systems) as compared to incidents involving wells (Folga et al., 2016). It appears that California's subsurface loss of containment (LOC) incidents are substantially higher than the worldwide average. A few of the California UGS subsurface incidents involved caprock integrity or leakage along faults arising from various causes, but only one reported instance of seismic damage of storage wells during an earthquake (CCST, 2018).

Damage due to permanent shear offset across wells has been documented associated with oil and gas production (e.g., at the Wilmington field in Long Beach until the 1960s (e.g., Dusseault et al., 2001) and at Belridge in the San Joaquin Valley (Fredrich et al., 2000). Almost all the well damage at Wilmington was associated with subsidence-induced bedding plane slip and low angle faulting in the caprock overlying the compacting reservoir. Casing impairment due to shear typically leads to loss of pressure integrity, pinching of production tubing, or an inability to lower workover tools. Historic observations of the effects of earthquakes in oil fields, such as from the 1983 Coalinga earthquake, suggest that ground shaking only impacts a very small subset of wells, primarily in the uppermost 100 meters (Hughes et al., 1990), while Hough and Bilham (2018) suggest that direct fault shear can cause severe well damage at depth. According to empirical fault scaling relationships, a moment magnitude (**M**) 5 event may involve shear displacement offsets of approximately 10 cm over a kilometer-sized fault rupture (Zoback and Gorelick, 2012). Such an event may not only rupture the wells intersected by the fault but could also perhaps create a permeable pathway along a fault through an otherwise intact caprock and thereby cause uncontrolled methane leakage.

Based on this historic assessment, a hypothesis may be that in terms of seismic impact on caprock and well integrity, permanent shear displacement of a fault intersecting or bounding the gas storage reservoir or overburden could cause substantial damage, as illustrated in Figure 1. Seismic shaking may cause less damage, but on the other hand shaking from one seismic event would impact a larger area and may be therefore more likely to hit a particular underground storage facility. A damaging fault shear activation may be less likely to occur in a particular underground storage facility, but if it happens the consequence may be greater in terms of well damage and potential gas leakage. The probabilistic seismic and fault displacement hazard analyses are part of the *OpenSRA* framework; the focus of Task C is on the potential damage caused by fault shear and ground motion.

Characterizing California Gas Storage Wells

There are hundreds of gas storage wells in California. Their typical configuration above the seal over the gas storage reservoir is shown on Figure 3 (the deeper portion is not subject to failure due to faulting that results in a gas release). Wells consist of borings and steel tubulars of different diameters, depths, wall thicknesses, and strengths. The annuli between the casings and rock or soil are cemented to varying extents.

Developing fragility curves involves multiple numerical modeling runs. This, given the duration of each run, makes developing a fragility curve for each well given all the variations infeasible. Consequently, a statistical analysis was carried out to identify the most common configurations. The analysis commenced by identifying gas storage wells open as of late 2019 that were not plugged or planned for plugging as of early 2021. The following data were entered from each of these well's records available for download from the California Geologic Energy Management Division (CalGEM) at that time:

- The diameter of each boring up to that for the production casing,
- The diameter, strength and grade of the casing installed,
- The maximum depth of each casing,
- The depth of the top of cement in the annulus around each casing, and
- The diameter, strength and grade of the tubing.

Assessing the statistical modes of the discrete parameters for casings and tubing proceeded pairwise. For example, the distribution of surface casing diameters corresponding to each production casing diameter. This enables identification of the top four well configuration modes, which are listed in Table 1.

Table 1: Top Four Well Configuration Modes

Mode Well API#	Surface casing				Production casing				Tubing			
	Diam. (in.)	Weight (lb/ft)	Strength (ksi)	Grade	Diam. (in.)	Weight (lb/ft)	Strength (ksi)	Grade	Diam (in.)	Weight (lb/ft)	Strength (ksi)	Grade
First	13.375	54.5	55	K	8.625	36	55	K	3.5	9.3	80	L
03721872	13.375	54.5	55	K	8.625	36	55	K	3.5	9.3	80	L
Second	10.75	40.5	55	K	7	23	55	K	3.5	9.3	55	J
01320115	10.75	40.5	55	K	7	23	55	K	3.5	9.3		
Third	13.375	54.5	55	K	9.625	47	80	N	3.5	9.3	80	L
03724130	13.375	54.5	55	K	9.625	47	80	N	3.5	9.3	80	L
Fourth	11.75	54	55	J	6.625	26		C	2.875	6.5	55	J
03714070	11.75	54			6.625	26		C	2.875		55	J

Each well configuration mode is followed by the American Petroleum Institute well number (API#) of a specific gas storage well in California with a configuration equal or close to that mode. API well numbers are unique identifiers for each well in the country. Note the two-digit state code 04 for California (04) starts the full API# but is not shown in the table.

Source: Sasaki et al. (2022)

The first, second, and fourth modes were selected for analysis of fault shear across wells and seismic shaking. The third mode was not included because it has the same surface casing and tubing as the first mode, but with a one-inch larger diameter production casing.

Table 1 does not include the extent of annular cementing. The presence or absence of cement in an annulus around a well casing is likely consequential to the probability of that casing failing due to shearing by fault movement. Surface casings are recorded as cemented along their entire length. Production casings are cemented along either a portion or all of their length from the base up. Only the facilities in the Coast and Transverse Ranges have Quaternary faulting in their vicinity. The modes selected for fault shear simulation are generally representative of wells in these facilities, which are slightly more susceptible to damage (for instance due to larger diameter tubing) than some wells that more closely match these modes. Including consideration of cemented and uncemented wells for each of the three selected modes, a total of six configurations were analyzed for fault shear across wells (Sasaki et al., 2022).

Table 1 does not include the extent and type of conductor casings. These are germane to a well's response to near surface ground shaking, which is generally stronger than at depth. Conductor casings are most commonly installed to a depth of 80 ft for the first and third modes, 40 ft for the second mode, and 33 ft for the third. For the first three modes the most common diameter is 20 in. installed in a 25 in. diameter boring. For the fourth mode the most common diameter is 18 in. in borings of unreported diameter. The full extent of annulus around the conductor casing is cemented.

Additional explanation of the well configuration statistics and their development are available in Sasaki et al. (2022) and Luu et al. (2022).

Figure 3: Typical Gas Storage Well Cross Section (Above Reservoir)

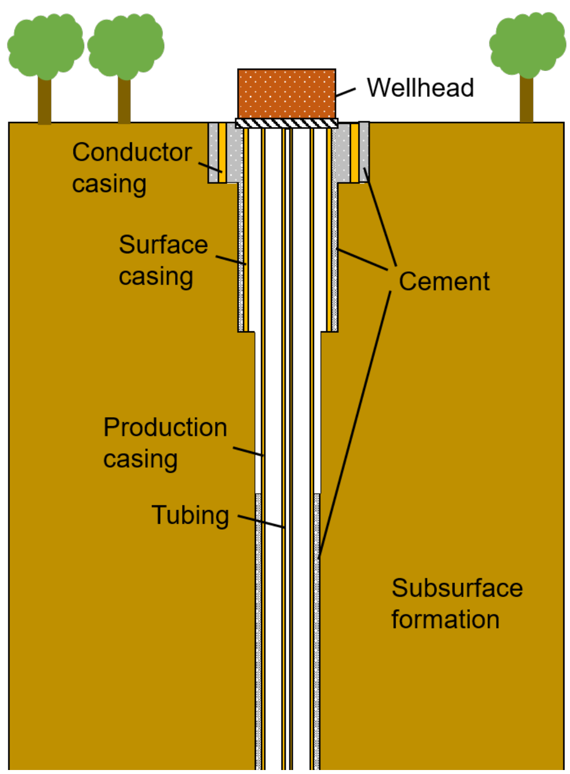

Only the portion of the well above the geologic seal over the gas storage reservoir is shown because damage to this portion of the well could release gas into the surrounding host rock and propagate to the ground surface.

Source: Sasaki et al. (2022)

Fault Shear across Wells

The objective of this subtask is to assess the range of fault displacements that could result in casing and/or tubing shear and rupture, in order to estimate the risk of well damage due to direct fault shear for various earthquake scenarios. To achieve this objective, a numerical model was constructed to simulate the behavior of a well-formation system during fault displacement, where the well-formation system comprises both the structural elements of the well and the subsurface formation that surrounds it. Details of the model and simulation methodology are provided in the following sections.

Numerical Model Geometry

Figure shows the geometry and boundary conditions of the well shear model. A commercially available geomechanics software, FLAC3D® (Itasca Consulting Group, 2020), was used for this modeling. The total depth range of the part of the subsurface formation that is modeled mechanically was 50 ft and the width and thickness were both 10 ft. Symmetry permits only half of the model thickness (5 ft) to be modeled. Hence, this is a local well-formation model, assumed to be located at a depth of 4,000 ft. The full model included the well section that extends from the ground surface to the well bottom located at 8,000 ft.

Figure 4: The Numerical Model for the Well Shear Simulation

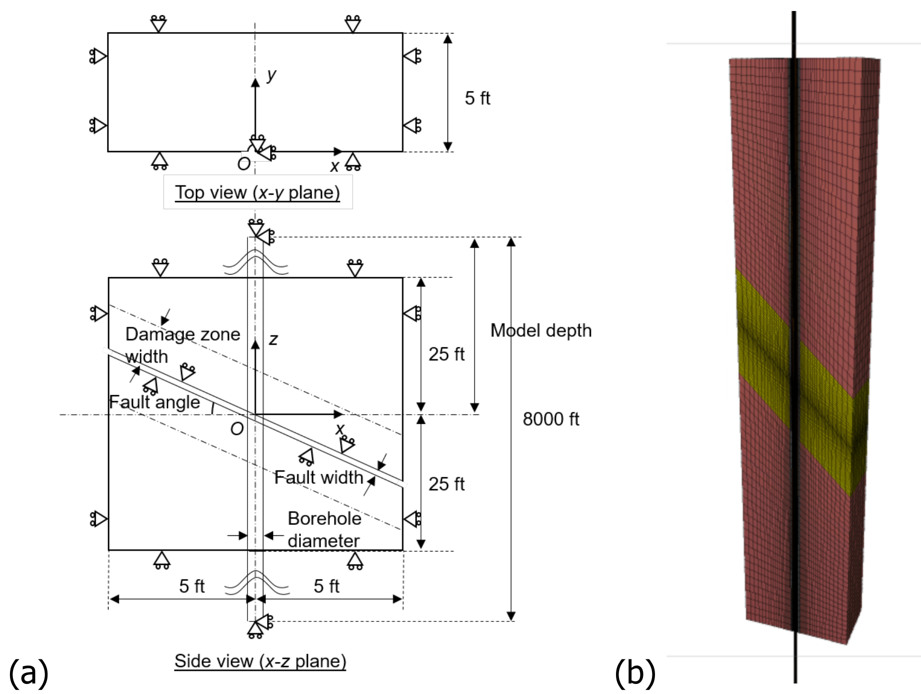

(a) The geometry and boundary conditions of the well shear model; (b) an overview of the model in FLAC3D (brown is intact rock, dark yellow fault zone)

Source: Sasaki et al. (2022)

The values of subsurface formation geometrical parameters, such as the fault angle and fault width shown in Figure 4b, were primarily estimated from expert opinion, and are assumed to follow log-normal distributions. The values of the well geometry parameters were determined from the well mode analysis described in the preceding section and are provided in **Error! Reference source not found.**.

Table 2: The Geometry and Strength Values of Well Components

	1st mode	2nd mode	4th mode
Borehole diam. (in)	12.25	9.875	10.625
Casing outer diam. (in)	8.625	7	6.625
Casing inner diam. (in)	7.825	6.366	5.791
Casing grade	K-55	K-55	N-80
Tubing outer diam. (in)	3.5	3.5	2.875
Tubing inner diam. (in)	2.992	2.992	2.441
Tubing grade	L-80	J-55	J-55

Source: Sasaki et al. (2022)

To include the uncertainty in the depth to the top of cement, two cement scenarios were considered for each well mode, cemented and uncemented annuli. In the former case, the gap between the borehole and casing was filled with cement, whereas in the latter case, the gap was left unfilled, and the fluid mud pressure was applied on the borehole and casing surfaces instead.

Material Constitutive Behaviors

The subsurface formation, fault zone and cement were modeled as elastic-perfectly plastic materials with a Mohr-Coulomb yield criterion. The casing and tubing were modeled as elastic-plastic, strain-hardening material with a Tresca yield criterion as shown in **Error! Reference source not found.**. The values of the mechanical parameters for the subsurface formation, casing, and tubing, were mainly estimated from in situ data and from the literature and were assumed to follow normal distributions.

Figure 5: Elasto-Plastic (Strain-Hardening) Behavior of the Casing and Tubing

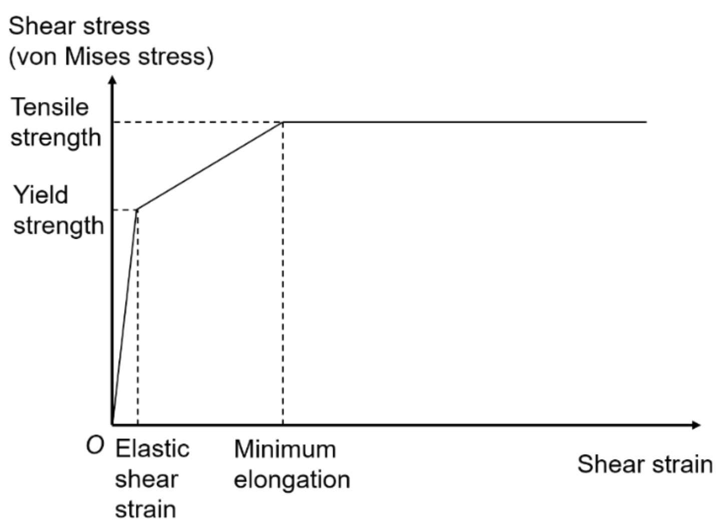

Source: Sasaki et al. (2022)

The interface behavior was simulated with FLAC3D's built-in contact model as shown in **Error! Reference source not found.**. The normal and tangential contact behaviors were modeled as linear strings with failure criteria (e.g., Coulomb friction in the tangential direction).

Figure 6: The Normal and Tangential Interface Behaviors

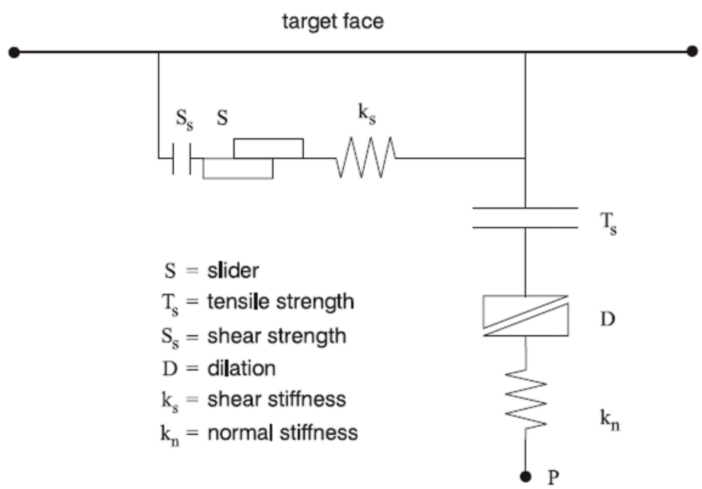

Source: Itasca Consulting Group (2020)

Well Shearing Process

The well shearing process was simulated by modeling reverse fault displacement as shown in **Error! Reference source not found.**; i.e., the portion of the formation above the fault m oved towards the upper left and the lower portion towards the lower right. Reverse fault displacement across wells would be the most likely scenario in California, though oblique strike-slip could also occur.

Figure 7: Boundary Displacements and Well Shear

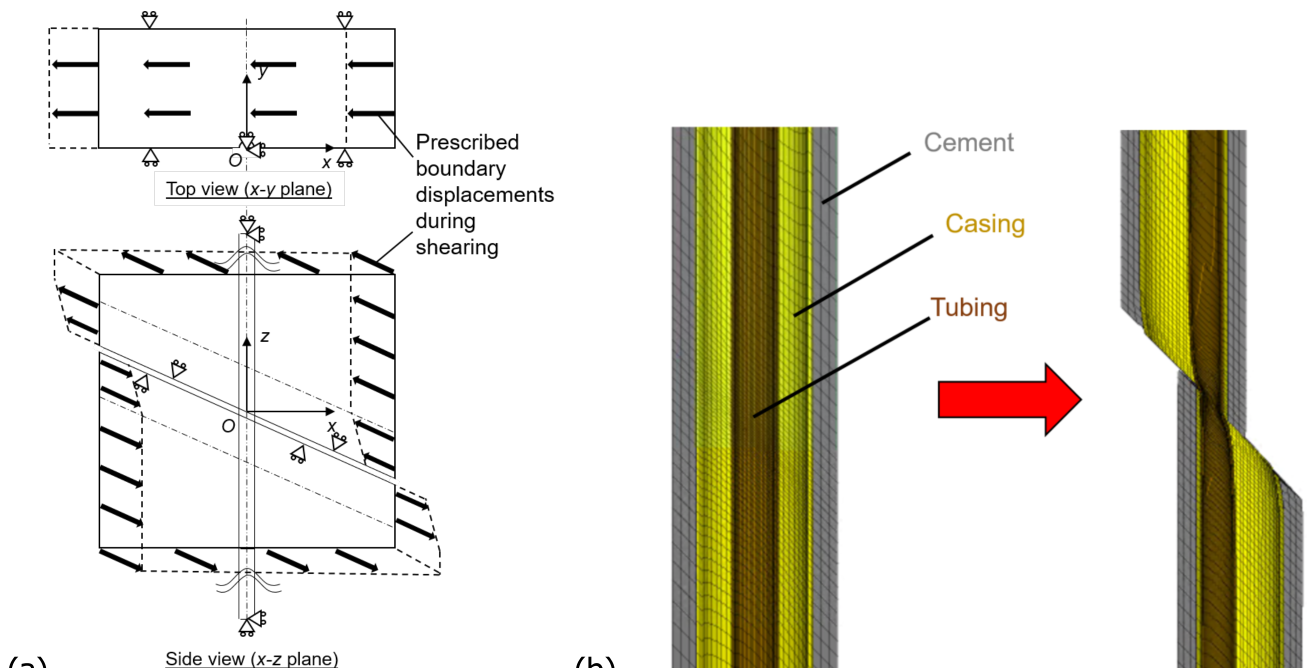

(a) Prescribed boundary displacement during shear; (b) Mesh deformation and rupture of casing and pinching of tubing during shear.

Source: Sasaki et al. (2022)

During well shearing, the rate of horizontal displacement on the model boundaries was fixed at 1.0E10^{-6} (m/s), so that the rate of vertical displacement changed with the fault angle. Also, the geometry of the model was updated every 1,000 cycles (i.e., every 1,000 sec) so that the large deformations/displacements due to fault offset were simulated. Finally, combined (non-viscous) damping, which is numerical damping whose magnitude is proportional to the unbalanced force (i.e., non-viscous) and direction is dependent on both the rate of unbalanced force and the velocity (i.e., combined), was used so that velocity oscillations during quasi-static rigid body motion would be suppressed.

Well Shear Sensitivity and Fragility Analyses

The sensitivity and fragility analyses were carried out to obtain the casing strain and tubing strain as a function of fault displacement as shown schematically in **Error! Reference source n ot found.**. The *y*-axis shows the maximum plastic shear strains in the casing and tubing and the *x*-axis is the fault displacement. At a specific casing strain limit, the casing was considered completely failed with a localized fracture simulated by removing numerical elements from casing (Figure 7b).

In total, the impact of 27 and 22 parameters on the well damage during well shear was investigated in the sensitivity analysis for the cemented and uncemented annuli scenarios, respectively. (The remaining five parameters for each uncemented case were either held constant or their sensitivity effects were accounted for by other parameters.) The results of the sensitivity analysis identified the critical parameters affecting well damage (i.e., accumulation of plastic shear strain), and the variability of only those parameters was incorporated into the fragility analysis to estimate how well damage varies with fault displacement. The results of the fragility analysis are provided in a later section of this report.

Figure 8: Outputs of the Well Shear Analysis

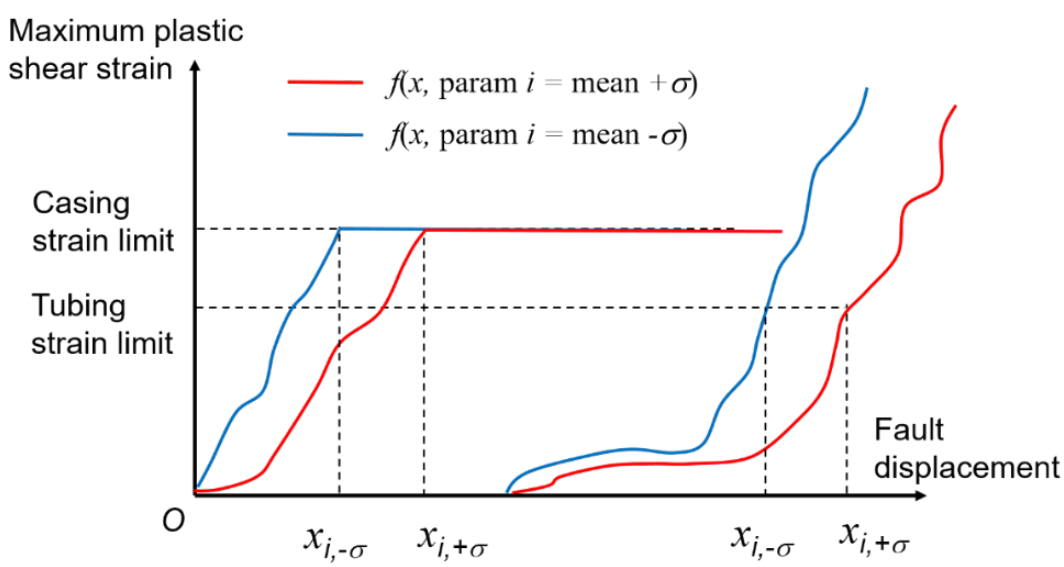

The red and blue curves indicate the maximum plastic shear strain profiles when the value of a single parameter (i.e., param i) was changed by +1σ and –1σ from its mean, respectively.

Source: Sasaki et al. (2022)

Dynamic Seismic Analysis of Well Integrity

This subtask aims to estimate the maximum bending moment a casing system sustains when subject to an earthquake-induced shaking excitation. To do so, a site response analysis (Kramer 1996) has been carried out to generate acceleration time histories at 2 m depth intervals as input ground motions for the dynamic simulations. The site response analysis was carried out using a 1D equivalent-linear method (Schnabel at al., 1972) due to its simplicity compared to nonlinear site response analysis (Idriss and Seed, 1968; Idriss and Seed, 1970). The Beam on a Nonlinear Winkler Foundation (BNWF) model has been implemented to evaluate the lateral response of the casing system embedded in a 1D layered soil profile and subject to an earthquake-induced excitation.

Equivalent-Linear Site Response Analysis

1D equivalent-linear site response analysis consists in estimating the magnitude of ground motion due to a vertically propagating seismic wave in a horizontally layered Earth model. It carries out an iterative linear analysis to approximate the nonlinear response of a site given a 1D soil profile. Several codes that implement the equivalent-linear algorithm already exist, such as SHAKE91 (Idriss and Sun, 1993), DEEPSOIL (Hashash et al. 2011), and Strata (Kottke and Rathje, 2009).

We carried out the equivalent-linear site response analysis using the code SHAKE91 to calculate both horizontal and vertical acceleration time histories at 2 m depth intervals using a selection of ground motions as "outcropping" motions. SHAKE91 requires the user to provide:

- The properties of each layer that composes the 1D soil profile, namely the thickness, the P-wave an S-wave velocities, the unit weight (or mass density) and the initial damping.
- The shear modulus reduction curve as a function of shear strain.
- The damping curve as a function of shear strain.
- The ground motion as acceleration input along with the layer where the ground motion is applied either as an "outcropping" or "within" motion.

Limited datasets are available for these parameters, and we selected the properties based on published papers and data. Sensitivity analysis studies over these parameters must be carried out to account for uncertainties. We used the mean curves from Idriss and Seed (1970) to describe the relationships between shear modulus reduction and damping as functions of shear strain. We used the velocities and densities of only the upper 60 m of the Los Angeles Basin 1D structural model[1], as the bending moments are expected to be the highest in the shallow subsurface due to the free motion of the attached wellhead (Ganpatye and

[1] https://strike.scec.org/scecpedia/BBP_1D_LA_Basin_Model

Ramamoorthy, 2019). Figures 9 and 10 show the shear modulus reduction/damping curves and the 1D soil profile used for the analysis, respectively.

The response of the soil profile to the input ground motion is returned by SHAKE91 in the form of acceleration and stress and strain time histories within the layers, and transfer functions at the interfaces. In this study, the ground motion is input at the first layer as "outcropping", and the acceleration time histories are output every 2 m along the soil profile and used as input ground motions for the seismic loading analysis.

Figure 9: Shear Modulus Reduction and Damping Curves

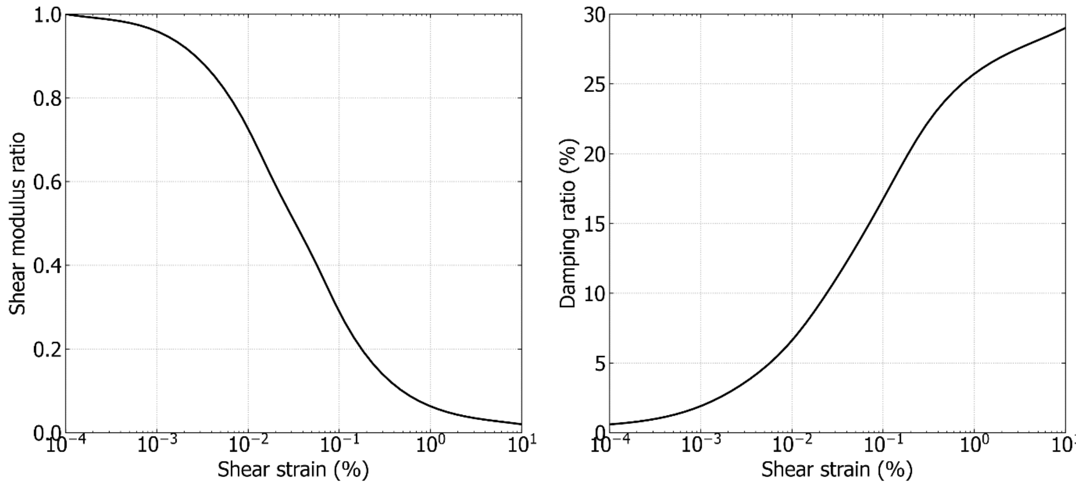

Source: Luu et al. (2022)

Figure 10: Velocity and Density Profiles

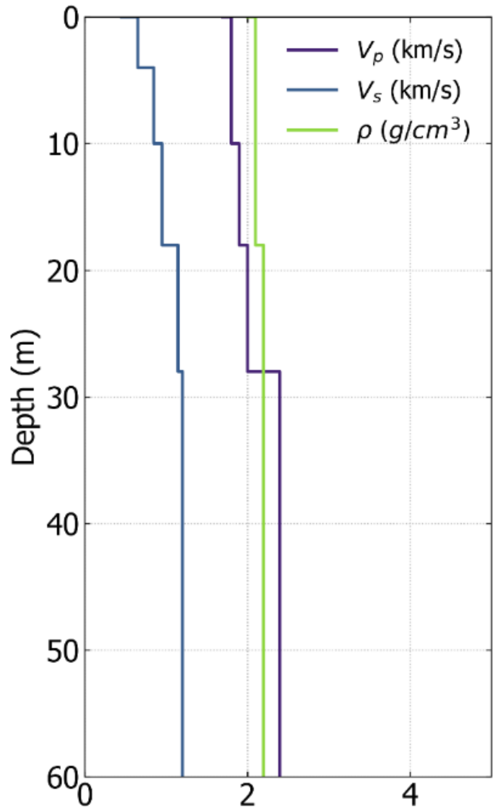

Source: Luu et al. (2022)

Seismic Loading Analysis

The response of a casing system to a seismic ground motion is strongly nonlinear and usually requires dynamic simulations to correctly account for the nonlinear behavior of the pipes. The BNWF approach is a simplified model where the pipes composing the casing system are modeled as a series of beam elements attached to nonlinear springs to represent the nonlinear pipe-soil interaction. Ground motions are then applied as boundary conditions to the springs' supports to account for the resistance of the soil.

We implemented this model into the open-source finite-element library OpenSeesPy v3.3 (McKenna 2011; Zhu et al., 2018). OpenSees is a software framework developed at the University of California, Berkeley, and has been widely used by the earthquake engineering community to simulate the structural response of geotechnical systems subject to earthquakes. Figure 11 shows the finite-element model used for the dynamic analysis in OpenSees.

Figure 11: Finite-Element Conceptual Model Used in OpenSees

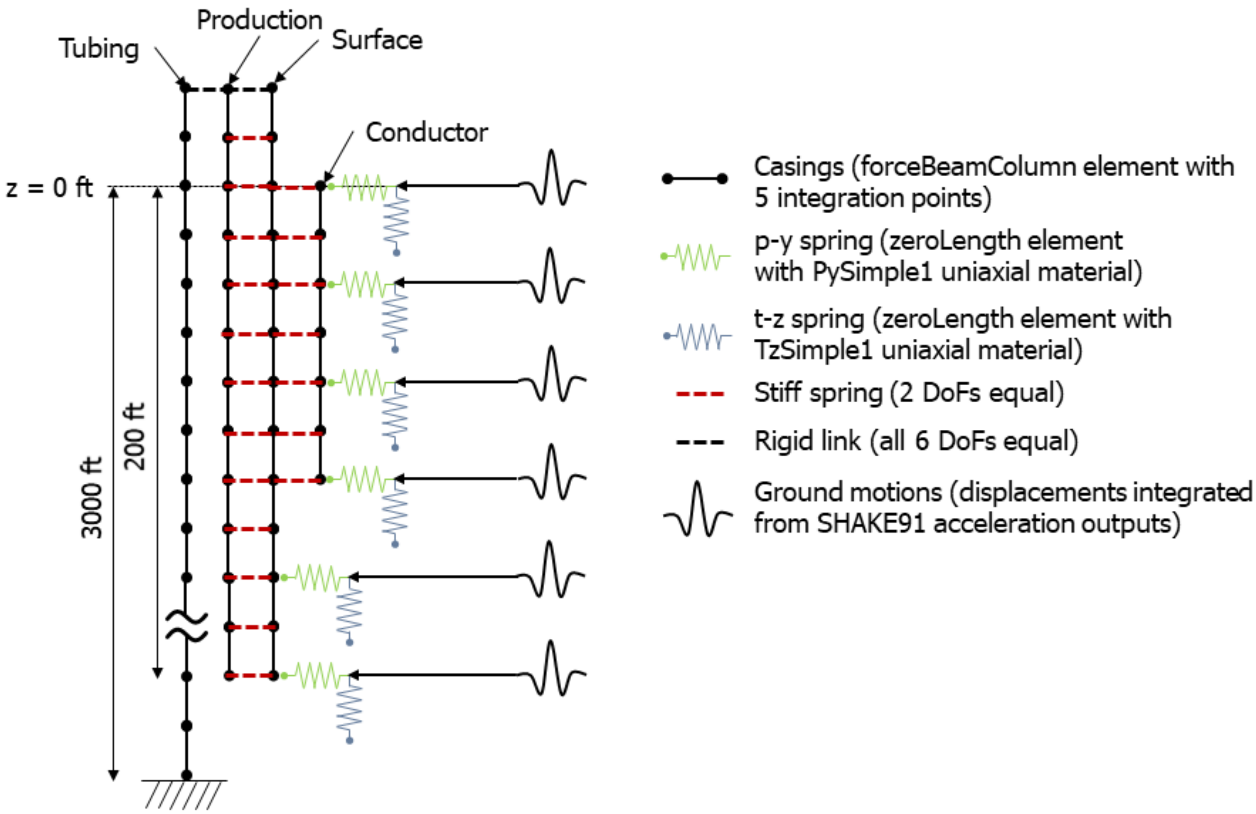

Source: Luu et al. (2022)

The different casings (conductor, surface, and production) and the tubing are modeled using Force-based Beam-Column elements using a Gauss-Lobatto integration method (Scott 2011) with 5 integration points. For the casings, only the top 200 ft (below ground surface) are modeled and discretized as 101 regularly spaced nodes; i.e., 100 2 ft long beam elements below ground surface. This is because the maximum bending of the casing occurs at shallow depths and rapidly decreases below 50-80 ft (Ganpatye and Ramamoorthy, 2019). For the tubing, the top 200 ft is modeled and discretized as 101 regularly spaced nodes as well and is extended down to 3000 ft and discretized by 101 additional nodes with the bottom node fixed. Above ground surface (i.e., wellhead), each beam element is 1 ft long. Each integration point of a beam element is modeled using a fiber section with a circular patch discretized into 16 fibers, each containing an OpenSees' *Steel01* bilinear uniaxial material for steel as shown in Figure 12. The interaction between the soil and the casing system is modeled using lateral (p-y) and axial (t-z) springs, which can be defined using zero-length elements with *PySimple1* and *TzSimple1* uniaxial materials in OpenSees, respectively. The wellhead and tree are not specifically modeled, but their mass is accounted for by increasing the mass at the nodes above the ground. Cement is modeled using stiff springs between the different cemented casings and the borehole. Acceleration time histories generated by SHAKE91 are applied as multi-support excitation patterns at each support node of the p-y and t-z springs (i.e., that are not attached to the casing system). A more detailed description of the properties of the different elements can be found in Luu et al., (2022).

Figure 12: Casing and Tubing Steel Model

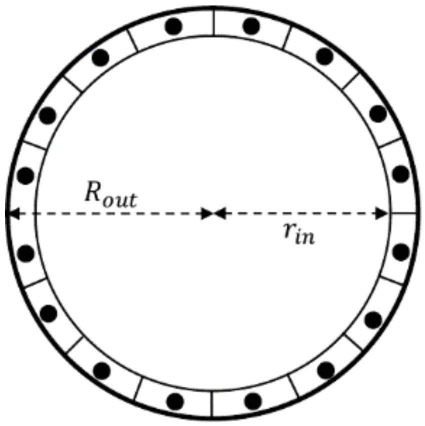

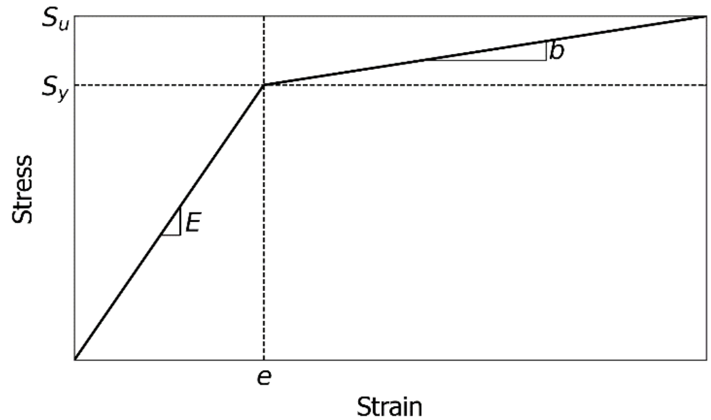

Casing and tubing modeled as beam elements in series consisting of fiber sections with circular patches (left) each containing a bilinear uniaxial material (right).

Source: Luu et al. (2022)

Following Ganpatye and Ramamoorthy (2019), we use the maximum bending moment to describe the capacity of a casing system to withstand lateral loading. In order to estimate the failure state of any pipe within the casing system, we define two damage metrics to represent the limit states expressed in terms of bending moment:

- Yield moment, defined as the bending moment at which the local stress in the pipe reaches the yield stress. When the maximum bending moment reaches this first limit, the corresponding cross-section starts to deform plastically. Beyond that limit, the plastic deformation is irreversible. Note that other parts of the pipe cross-section may be below yield with no plastic deformation.
- Plastic moment, defined as the bending moment when the entire cross-section of the pipe is above yield.

Caprock Integrity

Caprock integrity is an important part of the assessment of risks to a UGS facility, as it is the natural structure that contains gas within the reservoir. When an earthquake occurs, faults across the caprock could be activated, and as a result there could be a fault damage zone in the caprock with enhanced permeability. This zone connects the reservoir with the formations above, creating a leakage pathway for gas to migrate upward. If the storage reservoir is over pressured, reservoir fluid - gas and/or liquid - will have a driving force as well as a flow pathway to migrate upwards, leading to gas loss or other environmental issues.

The goal here is to develop a fragility curve that defines the relationship between shear fault displacement(s) during an earthquake and the damage rate of the UGS reservoir. There could be many definitions of a damage rate; here, the cumulative gas leakage after 30 years is chosen to be the damage rate. The reason for using a total leakage amount (vs. a leakage rate) is to capture the rate change due to dynamic changes in pressure over time. A cumulative leakage amount over 30 years is considered capable of capturing a leakage that causes concern, with a duration that is relevant to the operation of the facility.

As discussed above, the direct result of a shear activation is a change in fault damage and increased fault permeability caused by dilation and increased connectivity of fractures in the fault damage zone. The effect can be captured in one parameter, fault transmissivity - the product of permeability and flow area - as described below. To calculate the fragility curve, the first step is to establish a relationship between shear displacement and fault transmissivity. Then a numerical model is built to calculate damage rates resulting from changes in fault transmissivity. The second step is to assess the depth of and the pressure in a gas storage reservoir susceptible to leakage if a fault shears through the caprock seal. Finally, a suite of simulations is performed that considers uncertainties in fault transmissivity and some other parameters is performed to calculate fragility.

Shear Displacement and Fault Transmissivity Relationship

The permeability change that might occur during shear activation of a fault is highly uncertain. No established model exists for confidently making such a prediction. The approach taken here is conservative in that it considers a highly unfavorable scenario for potential leakage out of a storage reservoir. A model is proposed based on published research on permeability structures of faults in the shallow brittle crust along with observations of permeability variations in fractured rocks.

Fault zones are typically composed of distinct components (Cain et al., 1996):

1. A central fault core where most of the fault displacement is accommodated, and
2. a damage zone that is mechanically related to the growth of the fault zone.

The location of the fault core within a fault is shown in Figure 13. Typically, the core is near the center of the fault and within the fault damage zone. During a shear activation of a fault, most of the shear displacement occurs within the fault core. A fault core has generally low permeability and may act as a barrier to fluid flow. A damage zone is the network of subsidiary structures that bound the fault core and may enhance in-plane fault zone permeability relative to the core and the surrounding host rock. The permeability of the fault core is typically dominated by the grain-scale permeability of the fault rocks, whereas the damage zone permeability is dominated by the hydraulic properties of a fracture network.

In the case of a caprock above a gas reservoir, it is assumed that, if a fault exists and its flow transmissivity is initially low, the fault transmissivity could increase significantly during an earthquake when fault slip occurs. The amount of increase should depend on the magnitude of shear displacement. In general, shear displacement along a rough fracture may induce fracture dilation as a result of shear dilation that in turn would increase fracture transmissivity. This could be the case of activation along a minor fault consisting of a single conduit. In the case of a more mature fault, the shear displacement is usually observed to take place in the fault core. This fault core-localized shear could still enhance permeability in the adjacent damage zone. Here it is considered that the sudden shear slip in the fault core causes dynamic stress and strain changes in the adjacent damage zone that can stimulate the fracture network, increasing its permeability.

For calculation of gas leakage volume, it is assumed that fault slip above the gas reservoir would form a continuous path of enhanced flow transmissivity across the caprock. The total flow transmissivity of the flow path would be the permeability times the flow area. The permeability in this case is the damage zone fracture permeability, and the flow area can be estimated from the fault width (W) (i.e., width of the damage zone) and the length of the rupture (L) as shown conceptually in Figure 13.

The potential increase of fault permeability along a caprock fault is calculated based on damage zone permeability values that have been estimated and reported in the literature. A single large magnitude earthquake can cause damage over a relatively large distance on either side of the fault core, increasing the width of the damage zone. The upper limit for the fault damage width and rupture length corresponding to a slip event are estimated based on literature reviews.

Figure 13: Conceptual Model of Flow Area of an Activated Fault Crossing a Caprock

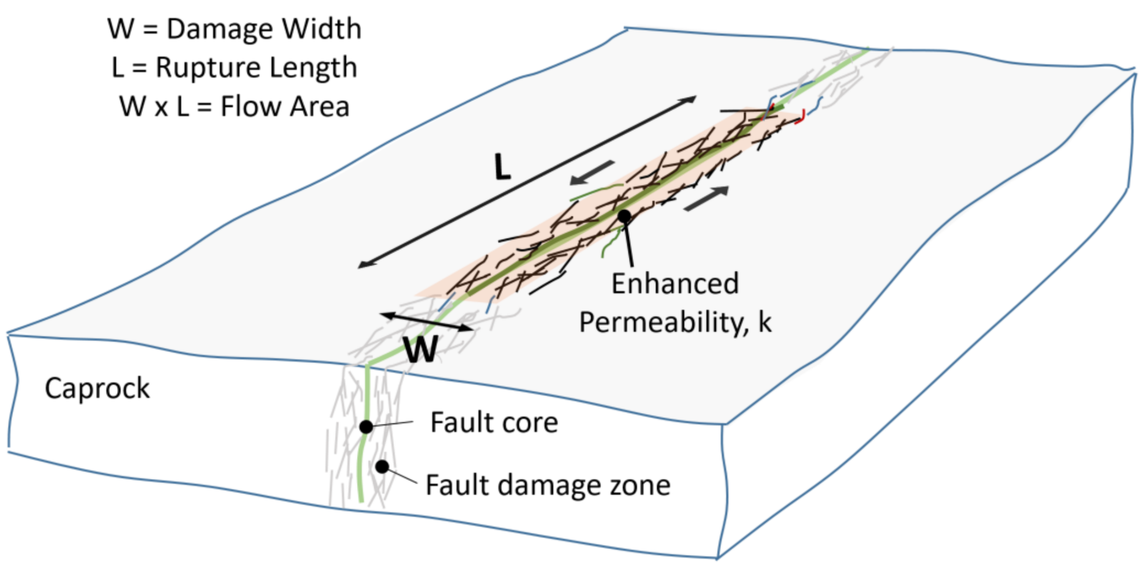

Fault transmissivity for vertical flow through the caprock is defined as the permeability multiplied by the flow area, where flow area is damage width (W) multiplied by the rupture length (L).

Source: Zhang et al. (2022)

Depth of and Pressure in a Reservoir with Seals Susceptible to Fault Shear

CCST (2018) assessed various risks to UGS facilities based on publicly available data. It identified wells at five facilities potentially crossed by Quaternary faults and categorized these as "likely" (Aliso Canyon and Kirby Hills), "maybe" (Los Medanos), and "unlikely" (Honor Ranch and La Goleta).

The depths of and pressures in gas storage wells at these facilities were collected from well construction records and monthly injection and withdrawal data available from CalGEM. The depth of the shallowest perforation, slot, or screen in each well was used as a proxy for the top of the reservoir. The monthly wellhead tubing pressures were converted to pressures at the shallowest opening of the well in the reservoir. This was done by iteratively calculating the gas density in the well via the gas formation volume factor approach in Guo and Ghalambor (2005). More details are available in Zhang et al. (2022).

Figure 14: Pressure in Facilities That May Have Quaternary Faulting

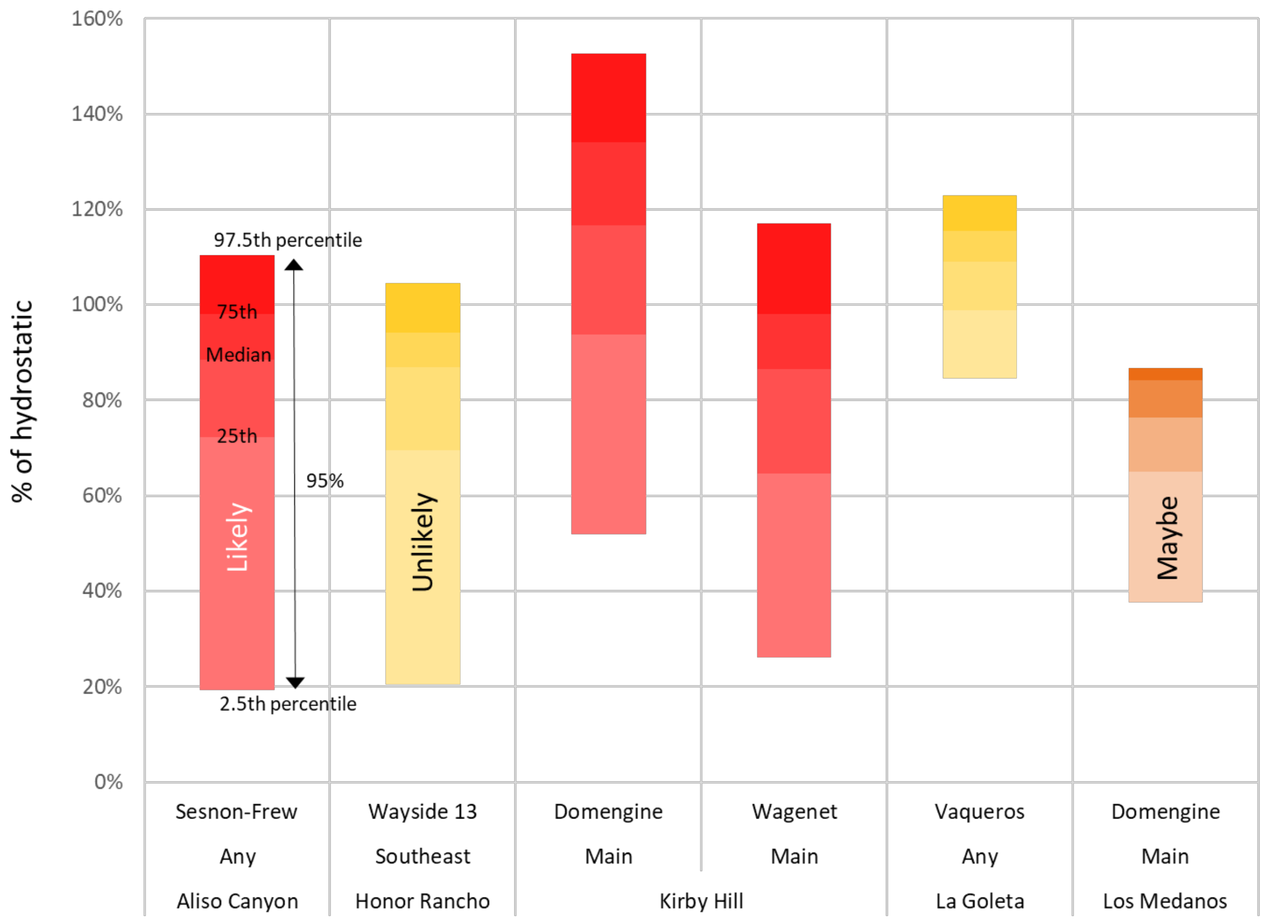

Statistics for reservoir pressure as a percent of hydrostatic in facilities having Quaternary faults in the vicinity. Reading the x-axis labels from bottom to top are the field name of the facility, the area within the field containing the storage reservoir, and the reservoir within that area. Coloring indicates judgement by CCST (2018) of the likelihood of a Quaternary fault intersecting wells in each facility.

Source: Zhang et al. (2022)

The downhole pressures were converted to percent of hydrostatic pressure to allow the pressures in wells of slightly different depths, across a facility due to structural relief, to be assessed. The resulting statistics are shown in Figure 14. These pressures are a good approximation of reservoir pressure because they are calculated from pressures during both injection and withdrawal. Further they were found to be almost exactly correlated between wells intersecting the original gas cap in the storage reservoir at Honor Rancho, irrespective of differences in direction or rate of flow. This suggests pressure losses due to flow in these wells is minimal.

For most gas storage reservoirs, pressure is generally below hydrostatic. This suggests that if a fault across a seal were to become transmissive due to slip, brine is more likely to flow into the reservoir than gas is to leak out. It would be relatively straightforward to withdraw a sufficient volume of gas to reduce pressure in the reservoir to below hydrostatic, as that is the normal condition.

The two exceptions are the Domengine reservoir in Kirby Hills and the reservoir in La Goleta. CCST (2018) judged it unlikely that a Quaternary Fault crosses through the La Goleta facility in the subsurface. This contrasts with Quaternary faults judged likely to cross the Kirby Hills field. The higher pressures in La Goleta are also considerably less than those in the Domengine reservoir at Kirby Hills. As such the latter reservoir was selected for further analysis (CCST, 2018).

Comparison of the distribution of pressures at each well in the reservoir by well depth found them uncorrelated. Therefore, the statistics for each given in Table 3 were developed independently.

Table 3: Depth and Pressure Statistics for Kirby Hills Domengine

	Mean	Standard Deviation
Depth (ft)	2144	81
Reservoir pressure (psi)	1042	254
Hydrostatic pressure (psi)	948	35

Source: Zhang et al. (2022)

Numerical Simulation for Fault Leakage Calculation

Simulation Software

The software we use for the study is iTOUGH2 (inverse TOUGH2), which is a computer program that provides inverse modeling capabilities for the TOUGH codes. The TOUGH ("Transport of Unsaturated Groundwater and Heat") suite of software codes are multi-dimensional numerical modules for simulating the coupled transport of water, vapor, non-condensable gas, and heat in porous and fractured media, developed at LBNL. iTOUGH2 has a fluid module appropriate for water and methane (EOSCH4) that suits this study. EOSCH4 models fluid properties for two components (water and methane) and two phases (aqueous phase and gas phase).

Numerical Model

In addition to enhanced fault permeability, another key factor that needs to be present for gas to leak out the storage reservoir is storage reservoir overpressure. Most of the UGS reservoirs in California are operated far below the hydrostatic pressure (Zhang et al., 2022). Even when caprock integrity is compromised due to an earthquake, gas may not leak out due to the lack of a driving force. As described above, the Kirby Hills Domengine storage zone is an exception to this. As given on Table 3, the mean pressure in this reservoir is 1042 psi compared to a mean hydrostatic pressure of 928 providing a mean overpressure of 114 psi. Note this is a rough estimate, without consideration of seasonal or yearly fluctuations.

Since the Kirby Hills Domengine storage zone operating pressure is most relevant for gas leakage risk compared to other UGS reservoirs in California, the Kirby Hills model geometries and parameters are used in the numerical model. Since a fault is a planar feature, a 2D model is considered sufficient for the purpose of the model. A schematic of the model is shown in

Figure 15. The model contains a UGS reservoir, a geological formation forming the caprock seal above the reservoir and a damage zone that connects the reservoir with the seal. The caprock matrix is not explicitly included in the model, since it is assumed non-conductive (i.e., zero permeability). Four scenarios for this model are considered in the next step to drive the fragility curve:

- Both the UGS reservoir and the formation above the caprock have open boundaries;
- Both the UGS reservoir and the formation above the caprock have closed boundaries;
- The UGS reservoir has open boundaries and the formation above the caprock has closed boundaries;
- The UGS reservoir has closed boundaries and the formation above the caprock has open boundaries.

The model parameters used here are summarized in Table 4.

Figure 15: The Schematics of the Numerical Model for Calculating Fault Leakage

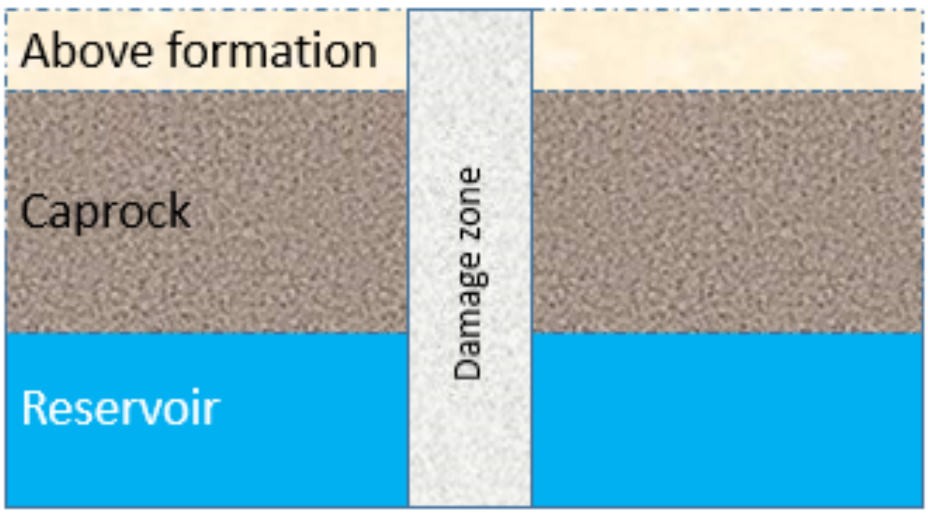

Not to scale.

Source: Zhang et al. (2022)

Table 4: Numerical Model Size and Input Parameters

Model geometry		**Reservoir parameters**	
Top reservoir depth (m)	600	Permeability (m^2)	2.e-14
Reservoir thickness (m)	120	Porosity	0.12
Caprock thickness (m)	200	Temperature (°C)	43

Source: Zhang et al. (2022)

Note this model is highly simplified with the following assumptions:

1. Properties (permeability, porosity) of each geological medium; the storage reservoir, damage zone, and the formation above the caprock (termed the "above formation") do not change over time.

2. Pressure and saturation in the gas reservoir is only affected by leakage through faults, and boundary condition do not change reservoir pressure, since operational activities (injection and withdrawal) are not considered.
3. Properties along the 3rd dimension (along-strike rupture direction in Figure 13) are the same as those in the 2D model, and the fault extends only to its rupture length L. Therefore, the total leakage amount can be calculated as the leakage amount from the 2D model multiplied by the fault rupture length L.
4. Leaked gas through the fault enters the formation above the caprock and will not continue to travel along the fault

The model output is the cumulative gas leakage over time.

Monte Carlo Simulation for Cumulative Gas Leakage Calculation

For the Monte Carlo simulations that are used to derive the fragility curve, the shear slip (Dslip), which affects the damage zone width (W) and fault rupture length, is a key variable in determining the total gas leak amount but is one of the uncertain parameters. In addition, other parameters are considered uncertain, including reservoir pressure, which determines the driven force for gas leak; reservoir gas saturation, which determine the amount of gas that is available for leakage; and fault properties that affect gas flow along the fault. The ranges of these parameters are summarized in Table 5. Most of the parameters are uniformly distributed within the specified range due to the lack of data to constrain the values, except the log(1/P0) in the Van Genuchten capillary function (Pruess, et al., 2011).

Table 5: Parameters and their Range

Uncertain parameter	Mean	Range
Dslip (m)	0.3	0.2 – 0.5
Pressure (Pa)	7.18e6	6.40e6 – 8.93e6
Reservoir Gas saturation	0.7	0.6 – 0.80
Log(Fault permeability(m^2))	-16	(-16) – (-14)
VG - Log (1/P0)[2]	-6.0	(-7) – (-5)
VG – m parameter[3]	0.45	0.3 – 0.6

Source: Zhang et al. (2022)

Because the goal of the Monte Carlo simulation is to derive the relationship between the gas leakage amount and Dslip, the range of the parameters are purposely selected to create gas leakage. For example, the reservoir pressure is set to be between the hydrostatic pressure,

[2] A parameter in the Van Genuchten capillary pressure function (Pruess, et al., 2011).

[3] A parameter in the Van Genuchten functions for both capillary pressure and relative permeability function (Pruess, et al., 2011).

and mean reservoir pressure plus its standard deviation, since the leakage is known to be zero if the pressure is below hydrostatic.

CHAPTER 3: Project Results

Results from the full-physics modeling related to (1) fault shear across wells, (2) ground motion impact on wells, and (3) potential caprock leakage along and activated fault is presented in the following subsections.

Fault Shear across Wells

Cemented Annuli Scenario

Results for the 1st well mode with cemented annuli are provided in Figures 16a and b. They show that the casing strains (Figure 16a) have a plateau at approximately 40% because the casing elements were removed at this strain level to simulate complete casing failure. In Figure 16b one can see that the tubing plastic strain is initially zero until a fault shear displacement of 0.1 to 0.2 m, because there is a gap between the production casing and tubing that needs to be closed by the casing deformation. It is noted that the critical strain level for the casing was determined from an API specification (API, 2018). It was found that the 1st mode casing ruptured when the fault offset reached somewhere between 1 to 3 cm. As for the tubing (Figure 16b), if the critical strain limit was set at 40% for comparison purposes, the fault offset needed for tubing rupture range between 15 cm and 28 cm.

Next, results for the 2nd mode provided in Figures 16c and d show that the casing ruptured at a fault offset of roughly 0.8 cm to 2.5 cm. These values are comparable to those of the 1st mode casing (i.e., 1 cm to 3 cm) despite the difference in the borehole (12.25 in vs. 9.875 in) and casing (8.625 in vs. 7 in) diameters between the 1st and 2nd mode, respectively. This shows that the borehole and casing geometries did not impact the magnitude of fault offset needed to rupture the casing if the annulus is cemented. The tubing failed (assumed at 40% strain) when the fault offset was somewhere between 11 cm and 21 cm. These values are less than those for the 1st mode tubing, due probably to the smaller gap between the casing and tubing [4.325 in (1st mode) vs. 2.866 in (2nd mode)]. However, the incremental fault offsets between the onset of plastic shear straining and 40% strain were rather similar [5 to 6 cm (1st mode) vs. 4 to 7 cm (2nd mode)]. This suggests that the tubing grade [N-80 (1st mode) vs. J-55 (2nd mode)] did not influence the development of tubing damage.

Finally, results for the 4th mode are provided in Figures 16e and f. The fault offset at which the casing ruptured ranged between approximately 1 cm and 2.5 cm, which did not significantly differ from those for the 1st and 2nd mode casing [1 cm to 3 cm (1st mode) and 0.8 cm to 2.5 cm (2nd mode)]. Hence, it was found that casings with different geometries and material grades ruptured at similar fault displacements as long as the annulus was cemented. The 4th mode tubing results show that plastic shear strain started to develop at fault offsets ranging between approximately 7 cm and 15 cm, and it reached 40% strain at a fault offset of approximately 10 cm to 22 cm. The incremental fault offset was thus 3 cm to 7 cm, which is comparable to those of the 1st and 2nd modes [5 to 6 cm (1st mode) and 4 to 7 cm (2nd mode)]

Hence, tubing with different diameters behaved essentially the same after the ruptured casing came into contact with the tubing.

Figure 16: Results of the Fragility Analysis (Cemented Annuli)

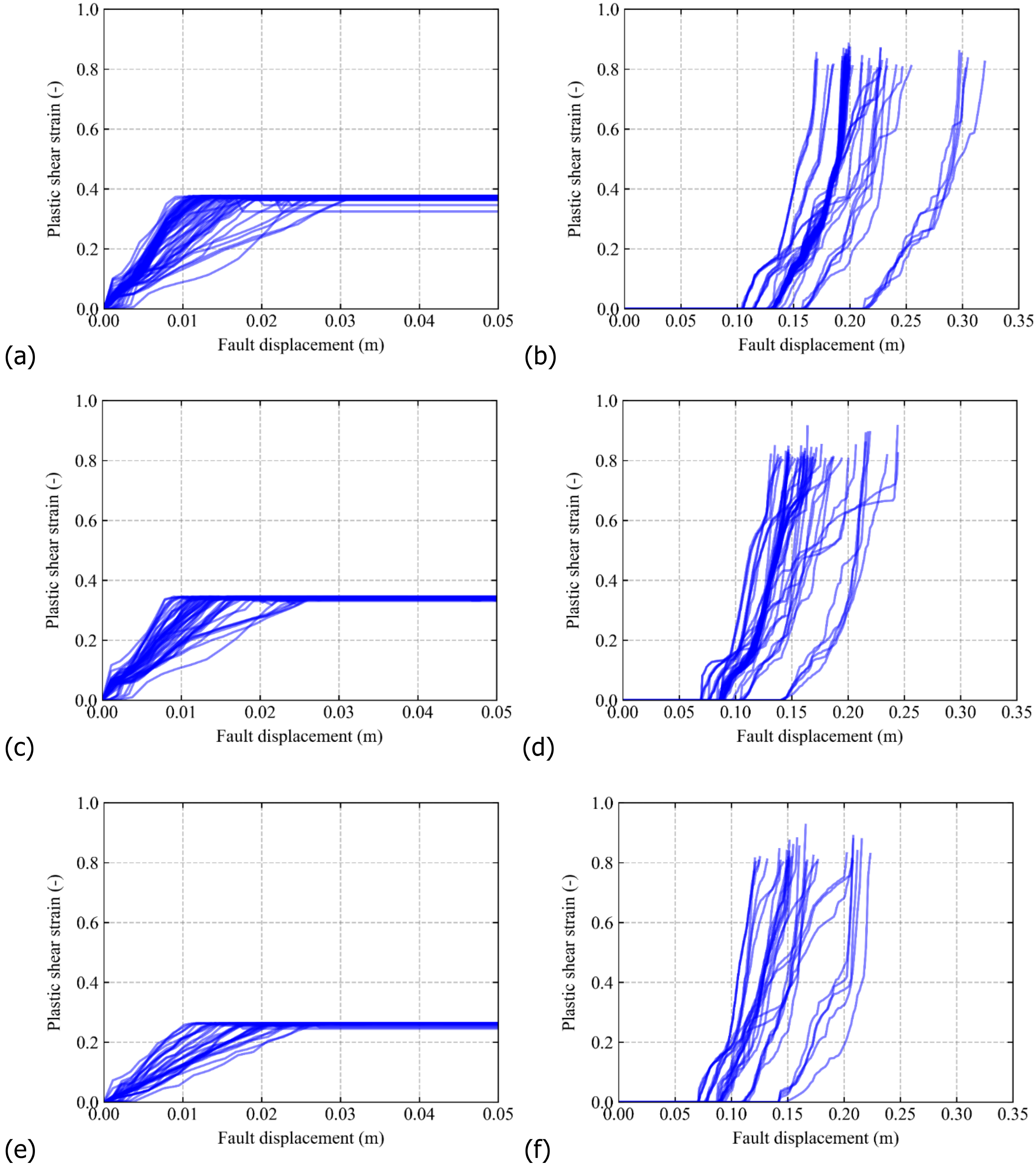

(a) 1^{st} mode casing; (b) 1^{st} mode tubing; (c) 2^{nd} mode casing; (d) 2^{nd} mode tubing; (e) 4^{th} mode casing; (f) 4^{th} mode tubing.

Source: Sasaki et al. (2022)

Uncemented Annuli Scenario

Results for the 1st well mode are provided in Figures 17a and b. The casing (Figure 17a) started to develop plastic shear strain at a fault offset of approximately 9 cm to 19 cm, and it reached the failure strain level at 14 cm to 28 cm. The incremental fault displacement between strain onset and rupture was thus 5 cm to 9 cm, which is significantly greater than that for the 1st mode with cement (1 cm to 3 cm). This is because it was easier to shear the casing with cement in the annulus than with the host formation alone. The incremental fault offset for the tubing ranged between approximately 5 cm and 7 cm (Figure 17b), which is in good agreement with that for the 1st mode (i.e., 5 cm to 6 cm). Hence, in contrast to casing shear, the tubing shear was not significantly affected by the presence of cement in the annulus.

Next, results for the 2nd mode are shown in Figures 17c and d. For the casing (Figure 17c), the incremental fault offset was approximately 4 cm to 7 cm, which is much greater than that for the 2nd mode with cemented annuli (i.e., 0.8 cm to 2.5 cm), as was the case for the 1st mode discussed above. Compared to the 1st mode without cement, the net incremental offset for the 2nd mode was slightly less, 5 cm to 9 cm (1st mode) vs. 4 cm to 7 cm (2nd mode). This indicates that the larger diameter casing in the 1st mode (8.625 in OD) resisted shearing slightly better than the smaller diameter casing in the 2nd mode (7 in OD). The incremental offset for the tubing was approximately 4 cm to 7 cm (Figure 17d), which is comparable to the 1st mode without cement (5 cm and 7 cm). This suggests that the tubing grade did not influence tubing shear, as the only difference between the 1st and 2nd mode tubing was its grade. The incremental fault offset was not much different (4 to 7 cm) from the 2nd mode with cement, indicating that the presence of cement did not essentially affect tubing shear.

Finally, results for the 4th mode are provided in Figures 17e and f. The incremental fault offset for the casing (Figure 17e) ranged from approximately 4 cm to 6 cm. These values are comparable to those for the 2nd mode without cement (i.e., 4 cm to 7 cm). The incremental offset for the tubing ranged between approximately 3 cm and 7 cm (Figure 17f), is similar to the 2nd mode without cement (i.e., 4 cm to 7 cm). This indicates that the smaller tubing diameter did not significantly affect its shearing behavior, as the primary difference between the 2nd and 4th mode tubing was the diameter, 3.5 in (2nd mode) vs. 2.875 in (4th mode) (the tubing grade was J-55 for both modes).

Figure 17: Results of the Fragility Analysis (Uncemented Annuli)

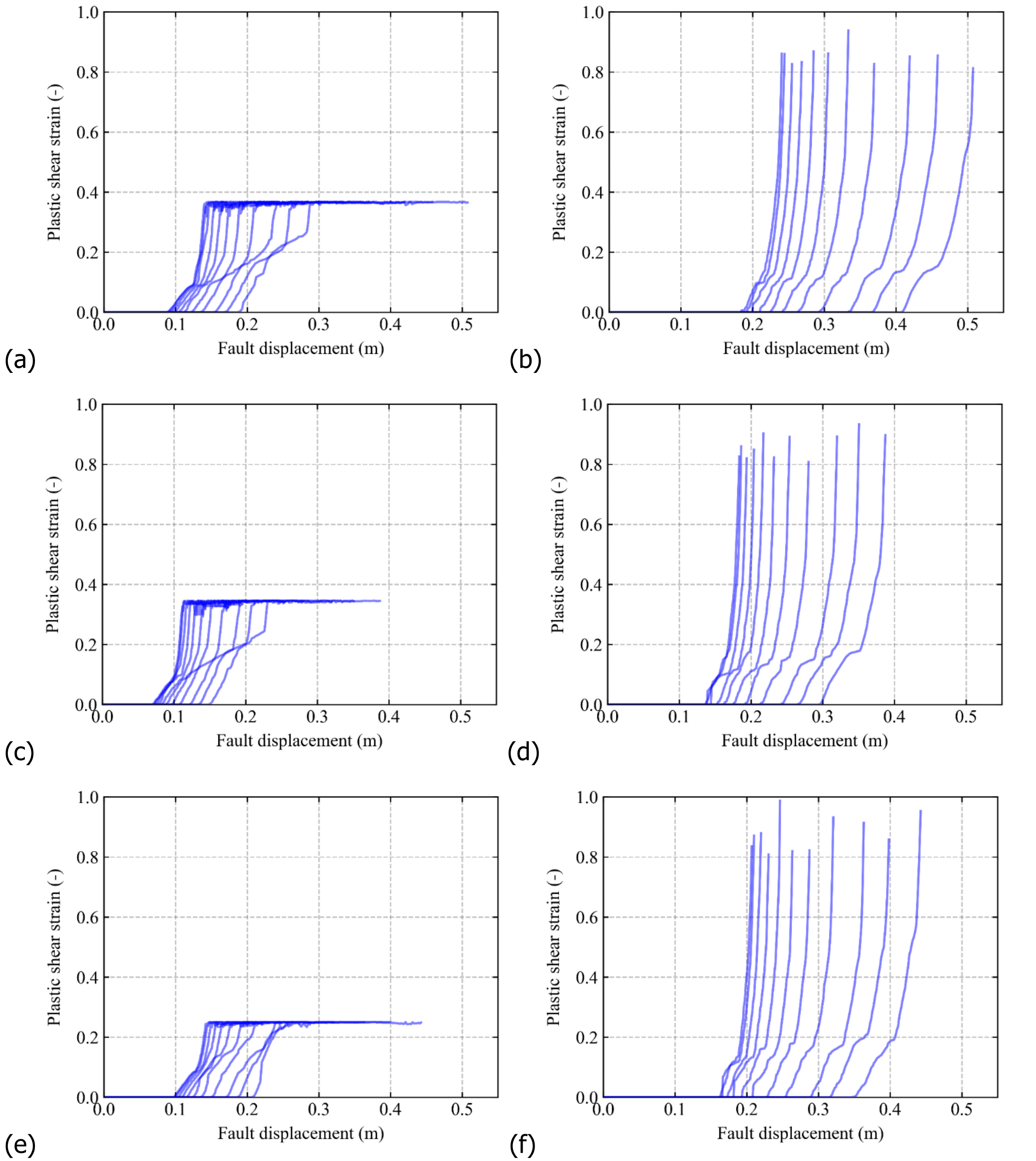

(a) 1st mode casing; (b) 1st mode tubing; (c) 2nd mode casing; (d) 2nd mode tubing; (e) 4th mode casing; (f) 4th mode tubing.

Source: Sasaki et al. (2022)

Fault Displacements at Casing and Tubing Rupture

Table 6 summarizes the fault offsets at which the casing and tubing ruptured for each mode. It is clear that the uncemented wells were able to resist greater fault displacements than the cemented wells, by as much as 1,300% for the casing, e.g., 1 cm vs. 14 cm (1^{st} and 4^{th} modes), and 100% for the tubing, e.g., 10 cm vs. 20 cm (4^{th} mode). Also, it seems that the 1^{st} mode well was able to resist fault displacement better than the other modes, whereas the 2^{nd} mode had the lowest resistance. This conclusion applies to both casing and tubing shear and regardless of whether the annulus was cemented or uncemented. However, this is largely due to the gap distances between borehole and casing and between casing and tubing. Hence, it is the well geometry, especially the gap distances, which had the greater impact on the fault displacements required to rupture the casing and tubing compared to the material properties.

Table 6: Fault Displacement at Casing/Tubing Rupture

	Fault offset at casing rupture	Fault offset at tubing rupture (40% plastic shear strain)
1^{st} mode	1-3 cm	15-28 cm
2^{nd} mode	0.8-2.5 cm	11-21 cm
4^{th} mode	1-2.5 cm	10-22 cm
1^{st} mode (without cement)	14-29 cm	23-49 cm
2^{nd} mode (without cement)	11-23 cm	17-37 cm
4^{th} mode (without cement)	14-26 cm	20-42 cm

Source: Sasaki et al. (2022)

Dynamic Seismic Analysis of Well Integrity

Ground Motion Data

Ground acceleration time histories used for the equivalent-linear site response analysis and applied at the top layer of the soil profile as "outcropping" motion, were provided by Slate Geotechnical Consultants and downloaded from the PEER Ground Motion Database. Each ground motion input consists of three separate acceleration time histories corresponding to the two orthogonal horizontal and the vertical components of ground motion. Figure 18 shows an example of the three ground motion components for a sample ground motion.

Figure 18: Sample Acceleration Time Histories

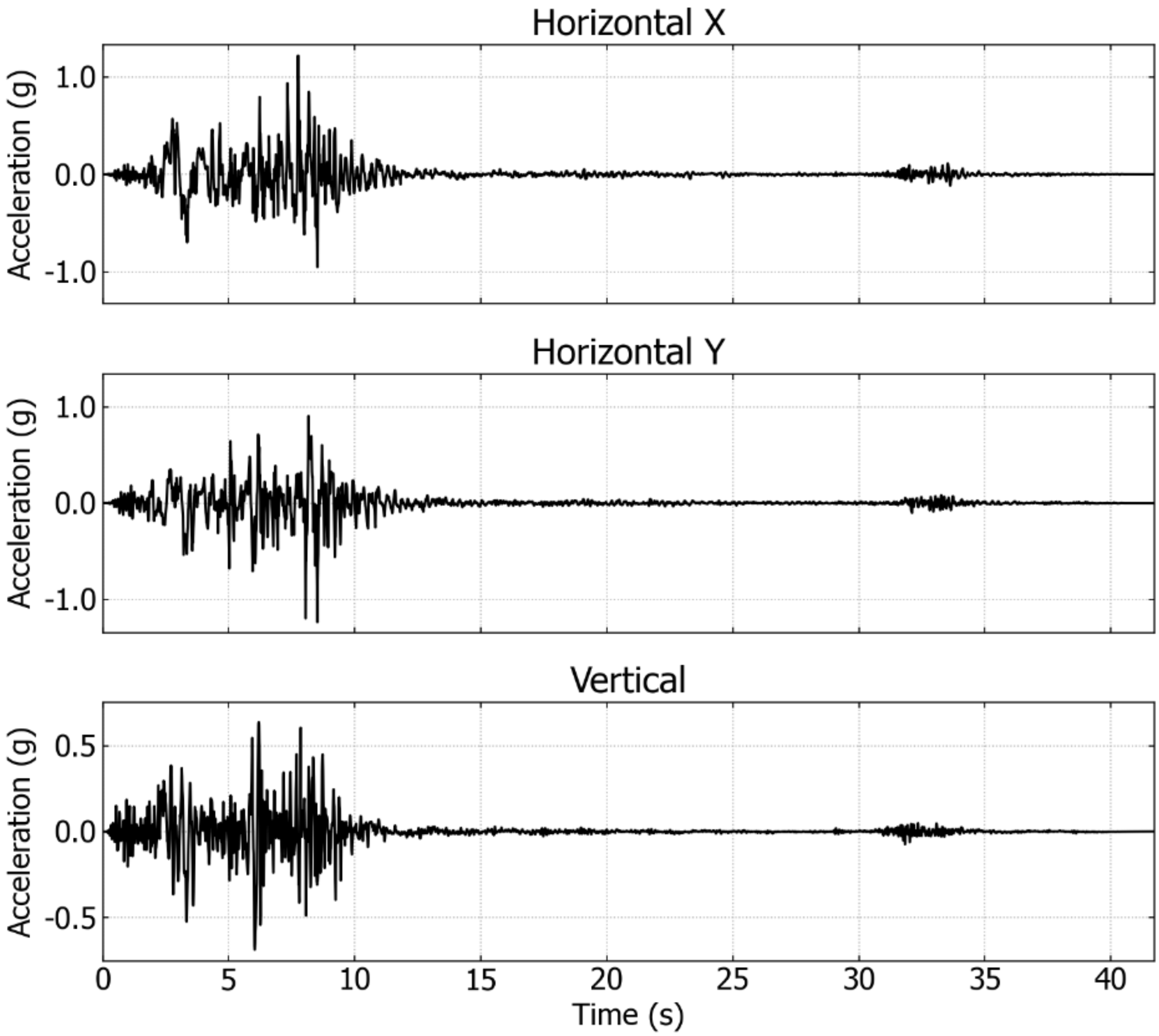

Source: Luu et al. (2022)

A list of the 60 acceleration time histories used in this study is available in Luu et al. (2022).

Equivalent-Linear Site Response Analysis

The goal of the equivalent-linear site response analysis is to generate a set of depth-dependent ground motions to be used for the seismic loading analysis for all the available input ground motions. This analysis is carried out using the code SHAKE91, which requires the user to provide the degradation curves (shear modulus ratio and damping ratio curves as functions of shear strain) and the 1D soil profile defining the P- and S-wave velocities, the mass density, and the initial damping for each layer. As discussed previously, due to the limited availability of datasets to develop the degradation curves and the soil profile, we carried out a sensitivity analysis to assess the uncertainties associated with these parameters. Results of the sensitivity analysis are described in Luu et al. (2022), and indicate that differences in the parameters for deeper layers are not expected to influence the maximum bending moments estimated for shallow depths (Ganpatye and Ramamoorthy, 2019).

For the 60 input three-component ground motions, we generated a set of horizontal and vertical acceleration time histories at 2 m depth intervals along the 60 m soil profile, resulting in a total of 30 depth-dependent time histories for each ground motion component. Figure 19 shows an example of three-component acceleration time histories output for all the 30 layers superimposed onto each other for a sample input ground motion.

Figure 19: Superimposed Acceleration of all Layers for a Sample Ground Motion

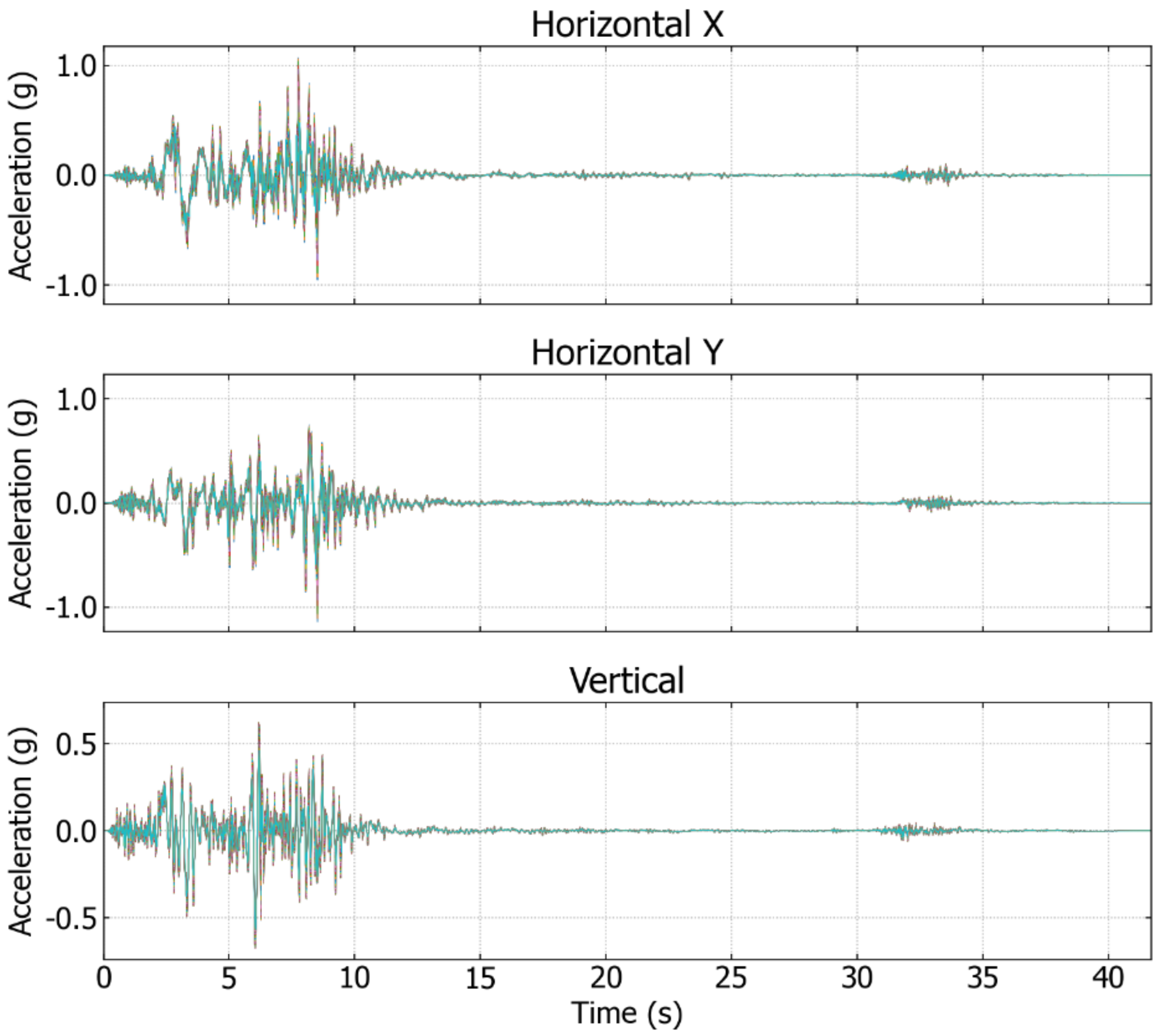

Source: Luu et al. (2022)

Seismic Loading Analysis

The seismic loading analysis aims to estimate the maximum bending moment the casing system is sustaining when subject to an earthquake-induced excitation. To achieve this, the depth-dependent acceleration time histories obtained from the equivalent-linear analysis are applied as time-dependent boundary conditions at the support springs that surround the casing system. For each input ground motion, the maximum bending moment for each of the three casings and the tubing is estimated using different combinations of model parameters. In order to develop reliable fragility curves, the parameter sampling should be sufficiently dense to cover the model parameter space.

The finite-element model implemented in OpenSees is controlled by a total of 24 parameters:

- 2 parameters for the soil: density and angle of internal friction.
- 2 parameters for the wellhead: height and mass.
- 5 parameters for each pipe: density, Young's modulus, Poisson's ratio, yield strength and yield-to-tensile strength.

We carried out a sensitivity analysis to determine the relevant model parameters for our simulation to reduce the number of parameters to sample, and consequently the total number of simulations to run. The sensitivity analysis showed that the maximum bending moments recorded along the casing system are primarily affected by a set of three parameters for all the casings and the tubing, namely the angle of internal friction of the soil, and the height and mass of the wellhead. In addition, the bending moment of the tubing is also sensitive to its Young's modulus and yield strength. In order to sample the parameter space for each ground motion and for the three well configuration modes, a set of 100 Latin Hypercube samples were drawn, resulting in a total of 100 x 3 x 60 = 18,000 simulations to perform.

Figures 20 shows the bending moment envelopes obtained for the three casings and the tubing for the three well configuration modes for a sample three-component ground motion. The bending moment envelope from each simulation is represented by a black thin line, and the thick green lines show the mean bending moment envelopes obtained by averaging the individual envelopes.

The dynamic simulations were carried out for the entire ground motion dataset. All the ground motions exhibit comparable results, and the following general trends can be observed:

- The maximum bending moment depends on the dimensions of the well and the peak acceleration of the ground motion.
- The maximum bending moment for the casings is located between 1 and 3 m below the ground surface.
- The maximum bending moment for the tubing is mainly located at its top, above the ground surface.
- The maximum bending moment decreases rapidly below a depth of approximately 5-7 m.

These observations are consistent with the observations reported by Ganpatye and Ramamoorthy (2019) for the Aliso Canyon gas storage field.

Figure 20: Results of Seismic Loading Analysis for a Sample Ground Motion

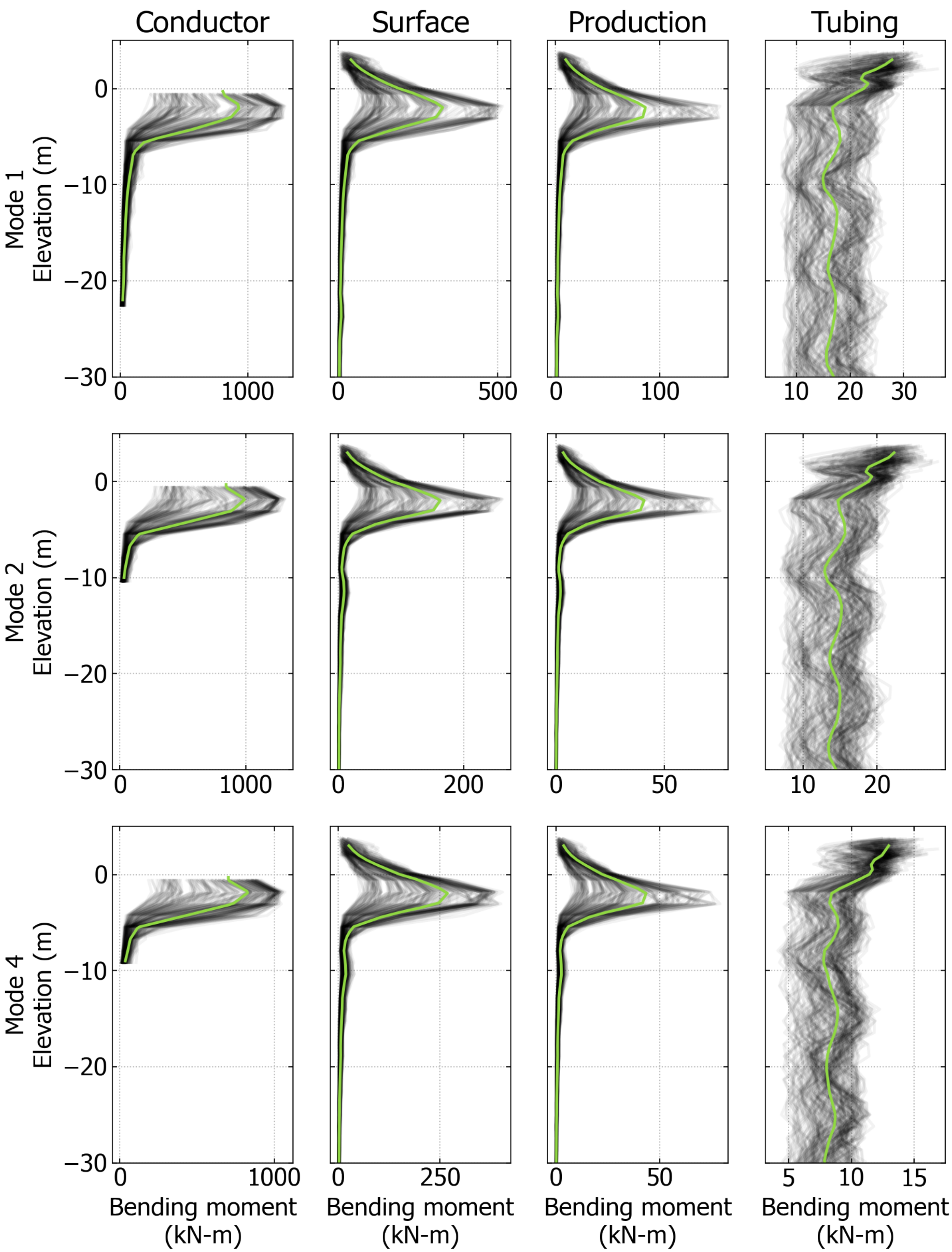

Source: Luu et al. (2022)

For all the ground motions, the maximum bending moments recorded along each component of the casing system have been provided to Slate Geotechnical Consultants to develop the fragility curves, which will be available in an upcoming publication.

Caprock Integrity

Results for this section include:

- A relationship between fault shear displacement (Dslip) and fault transmissivity
- A set of example simulations showing the evolution of the gas leak rate
- Monte Carlo simulation results showing a relationship between Dslip and the cumulative amount of leaked gas at 30 years

Relationship Between Fault Shear Displacement and Fault Transmissivity

Very few data exist on fault permeability enhancement caused by slip events. The main literature to guide the derivation of the relationship between fault slip and enhanced permeability includes:

- Fault damage zone permeability estimates in the range of 1e-15 to 1e-14 m^2 (e.g., Wibberley and Shimamoto, 2003)
- Observed increases in permeability associated with stimulation of tight shale gas reservoirs in the range of 1e-15 to 1e-14 m^2 (e.g., Salem et al., 2022)
- Studies of fractured shale in the laboratory with measured permeability up to 1e-14 m^2 (e.g., Yang et al., 2021).

Based on such field and laboratory data, an upper limit of 1e-14 m^2 for fault damage zone permeability is adopted.

Estimation of the flow area along the fault is based on the review and compilation of data from numerous published sources by Torabi and Berg (2011), shown in Figure 21. Here, the empirical fault scaling relations derived from the data are used to relate fault shear offset to the generated width of the damage zone and to the rupture length. It should be noted that the empirical relations between fault offset and fault width in Figure 21a are based on the cumulative shear offset over geologic time, but, due to the lack of information in the literature, this relation is conservatively applied here to single-event displacements. Moreover, the width of the damage zone is not a well-defined parameter. However, it is the portion of the damage zone closest to the fault core that will sustain the largest damage and permeability enhancement.

The following approximate empirical relation between fault shear displacement, Dslip, and width, W, is apparent from Figure 21a:

$$W = Dslip \times 1 \qquad (3.1)$$

That is, the zone impacted by damage is estimated to be equal to the shear displacement of an earthquake. Based on Figure 21b, the single-event rupture length L for a given Dslip can be roughly estimated as shown in equation 3.2.

$$L = Dslip x 10{,}000 \qquad (3.2)$$

Figure 21: Fault Scaling Relations from Literature

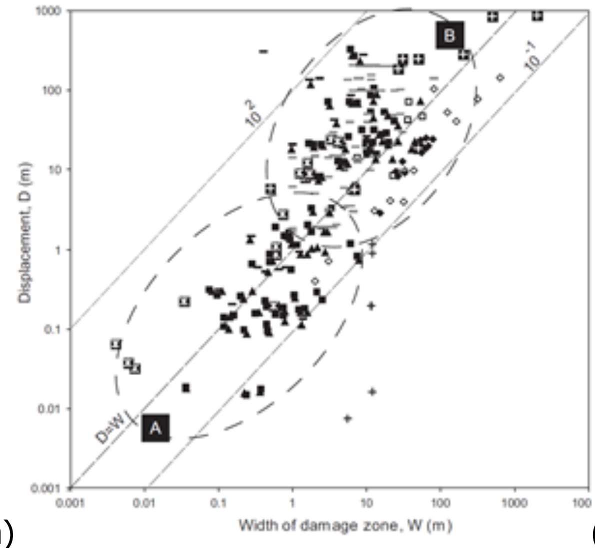

(a)

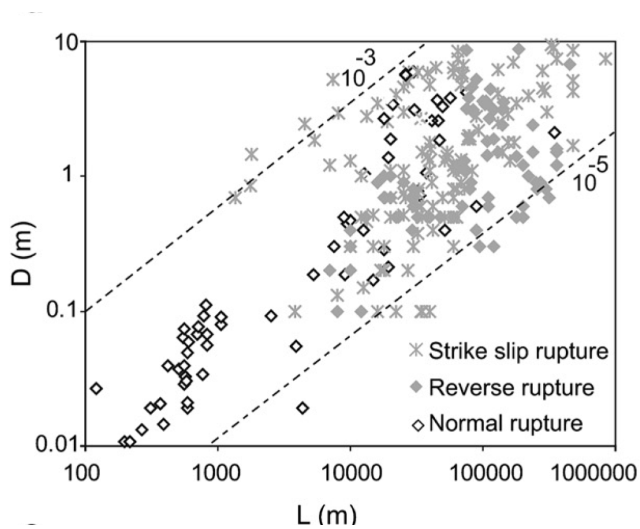

(b)

(a) Cumulative displacement versus damage zone width for siliciclastic rocks. The data show two slightly different distributions for small (subset A) and medium-size faults (subset B). (b) D–L relationship for single-event earthquake ruptures.

Source: Figures from Torabi and Berg (2011)

The fractured rock permeability is assumed to remain high for some time after activation. However, if the host rock is weakly consolidated and has a high clay content, fractures may not stay open, but close and seal as a result of high confining stress and/or swelling. Moreover, fractures in weakly consolidated rocks and ductile shale may not dilate during shear. In fact, faults in weakly consolidated rocks may completely lack a damage zone.

To summarize, conservative estimates for potential gas leakage amounts in the next section are based on the following assumptions:

1. Fault activation will cause the creation of continuous flow transmissivity along the fault damage zone that crosses the caprock.
2. An upper limit of 1e-14 m^2 for the enhanced fractured rock permeability at the depth of a gas storage facility.
3. The width (W) of the zone of enhanced permeability increases with the magnitude of shear slip according to W = Dslip, which is considered an upper limit.
4. The length of the fault rupture (L) and the length of the zone of enhanced permeability increases with shear slip according to $L = Dslip\ x\ 10{,}000$.
5. The enhanced permeability of the damage zone will persist, and the zone will not seal over time, which provides an upper limit for potential gas leakage.

Overall, these are all conservative assumptions. In particular if the caprock consist of weakly consolidated host rock and of high clay content, fault activation may not result in any significant permeability enhancement.

A Set of Simulations Showing Gas Leak Rate

To demonstrate how the gas leak rate evolves over time and investigate the impact of the reservoir and formation boundary conditions, a set of parameters are selected to ensure gas is able to leak out of the storage reservoir in four scenarios. Although the damage rate is defined as the cumulative amount of gas leaked at 30 years, this set of simulations are run to 100 years. Gas and liquid flow rates at two points on the fault, from reservoir to fault, and from the fault to the above formation are shown in Figure 22.

Figure 22. A Set of Simulations Showing Evolution of Gas Leakage Rate

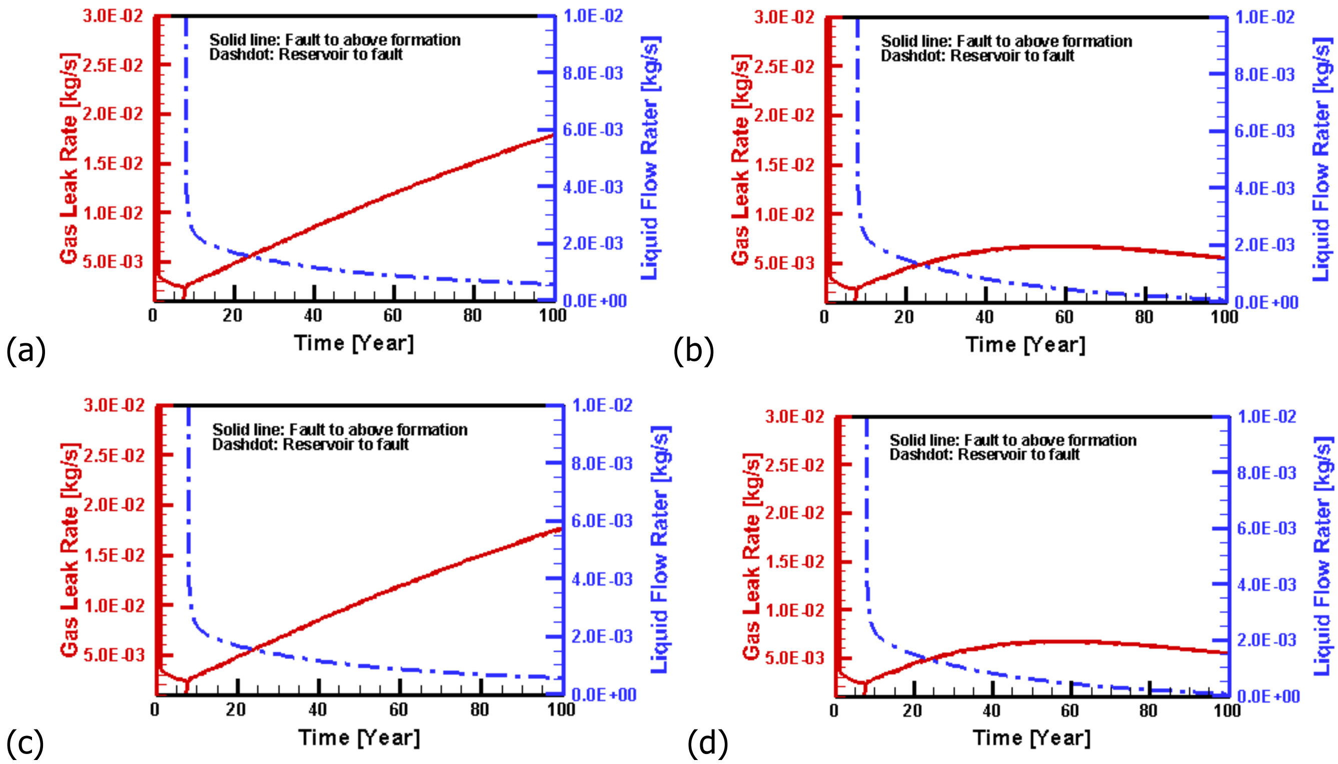

Gas leak rate and liquid flow rate for scenarios (a) both UGS reservoir and the above formation have open boundaries; (b) UGS reservoir has open boundaries, and the above formation has closed boundaries; (c) UGS reservoir has closed boundaries and the above formation has open boundaries; (d) Both UGS reservoir and the above formation have closed boundaries. Solid red/blue lines show gas/liquid flow from the fault to the above formation; dash-dot red/blue lines show gas/liquid flow from reservoir to fault.

Source: Zhang et al. (2022)

The following observations are made based on the set of simulations:

- There is not much difference between the gas flow rate from reservoir to fault, and the rate from fault to the above formation once the gas flow is established (the two lines are almost overlaying each other so the dashed-dot curve is hard to see). However, it is possible (not shown here) that a small amount of gas flows into the fault from the reservoir due to capillary pressure, when there is not enough overpressure, and dissolves into the liquid in the fault; in this scenario a gas flow within the fault or from the fault to the above formation is never established. Those simulations are not relevant to leakage and are therefore not shown here. As a result, it is determined that the cumulative gas flow from the fault to the above formation is used for damage rate in the Monte Carlo simulations.

- For this set of simulations, a significant amount of liquid water is initially leaking from the reservoir to the fault due to the significant overpressure (hydrostatic pressure plus a standard deviation) applied in the reservoir, and to the initially fully liquid saturated fault. As time goes on, more and more gas flows into the fault, the relative permeability of gas in the fault increases and the gas leak rate increases. The liquid water flow at the point between the fault and above formation is a small negative value, meaning a reversed flow, i.e., very little liquid flow is observed from the above formation to the fault. Although not demonstrated from this set of parameters, it is possible to have a more significant liquid flow from the formation above to fault, eventually establishing a liquid flow from fault to reservoir over (a long) time.
- The boundary conditions on the reservoir have little impact on liquid flow rate, as the liquid leakage from the reservoir is not significant for the simulated period compared to the total storage in the reservoir, or the reservoir size is so large that the conditions at the boundaries are not affected by the small leakage. However, the volume of the formation above the caprock is less than a tenth of the reservoir volume (the thickness is set at 10m to mimic a fast flow path). In scenarios (b) and (d) in Figure 22 the pressure increases at 40 years of gas and liquid leakage and thereafter is large enough to stop the gas leakage rates from increasing, or even to cause them to reduce at later times. Since the damage rate is defined as the cumulative gas leaked at 30 years, the Monte Carlo simulation results are expected to be the about the same for all scenarios, based on Figure 22. Therefore, the Monte Carlo simulations only need to be performed for one of the scenarios, chosen as scenario (a) in Figure 22.

Monte Carlo Simulation Results

A total of 500 Monte Carlo simulations were performed. Among those only 91 resulted in gas leakage into the formation above the caprock. Figure 23 is a plot of each parameter vs. damage rate (i.e., total gas leak) for those 91 simulations.

A linear fit is made for each data pair. Among the parameters, four of them, Dslip, reservoir over pressure, log(permeability) and the m parameter show a distinct (if rather poorly constrained) trend. These are relative influential parameters in that they have a significant impact on total gas leakage. Fault permeability shows a clear cut at -14.7, i.e., gas leaks out of the fault only if the fault permeability is above 2.e-15 m^2. It is clear that this is the most influential parameter. Change in reservoir gas saturation (Figure 23c) and log (1/p0) (Figure 23d) do not seem to have a significant impact on the gas leakage.

It is reiterated that these simulations are based on a lot of underlying assumptions, so that the results are highly uncertain. In actual practical applications, it will be very important to include as much site-specific information as possible to make more realistic assessments.

Figure 23: Monte Carlo Simulations that Resulted in Gas Leakage

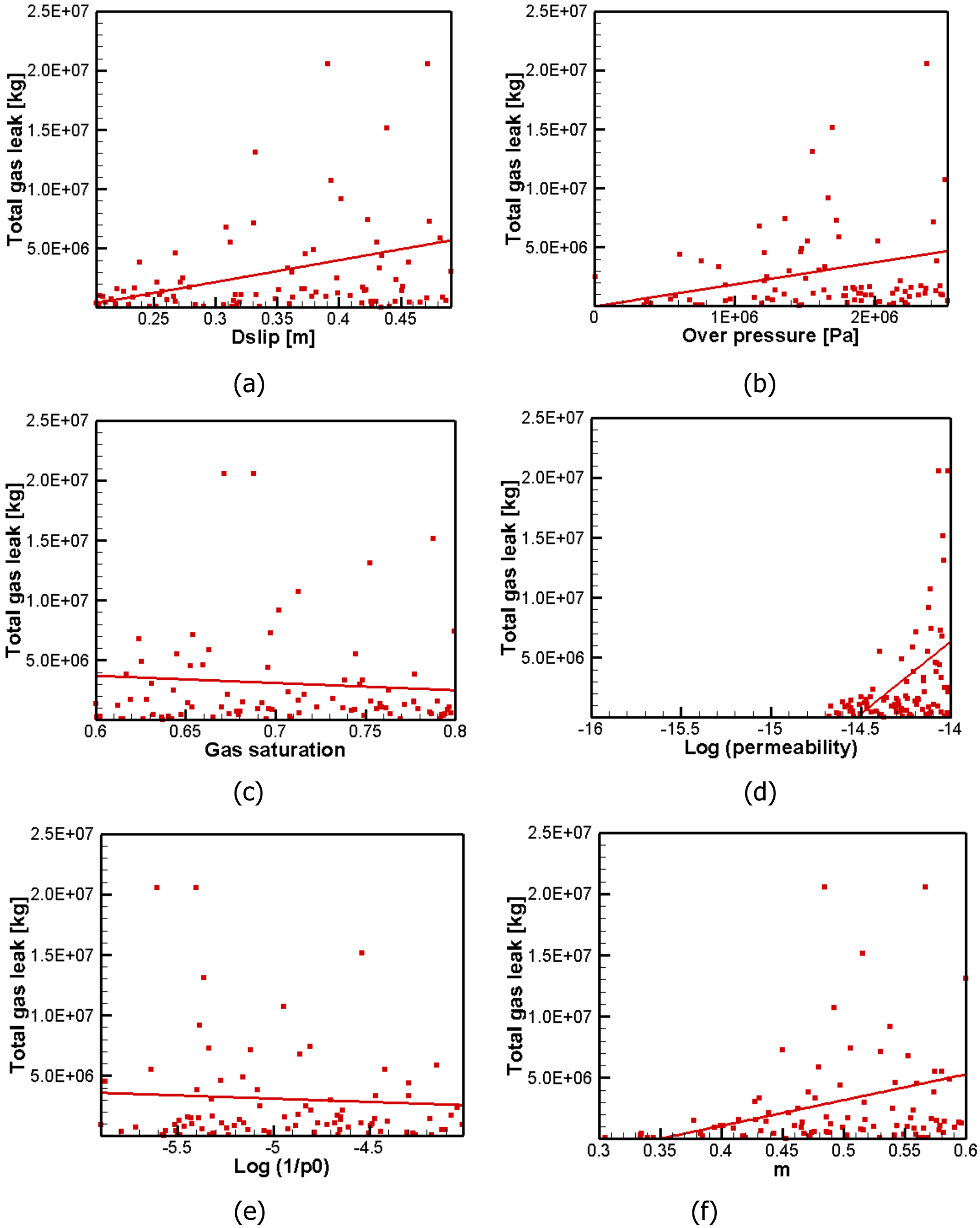

Figure shows the relationship between each parameter and total gas leak age: (a) Dslip; (b) reservoir overpressure; (c) change in gas saturation; (d) log(permeability); (e) log(1/p0); (f) m parameter. Data points are taken directly from the simulation outputs. Lines are linear regression fits to the data.

Source: Zhang et al. (2022)

CHAPTER 4: Conclusions/Recommendations

This report summarizes targeted research on seismic impact on wells and caprocks associated with underground gas storage facilities, with the ultimate project goal of advancing the seismic risk assessment tool, *OpenSRA*. The research has been divided into three subtasks related to

1. direct fault shear displacement across wells,
2. ground motion (shaking) impact on wells, and
3. potential caprock gas leakage.

The work under these three subtasks was preceded by a literature review of historic data and events related to seismic impact on wells and underground gas storage facilities. The characteristics of California gas storage facilities were reviewed using public records of operating pressures, depths, and well designs. In particular, statistics of California gas storage wells were collected from public records to characterize them into four main well designs to be investigated for seismic impact. In each of the three subtasks, advanced full-physics modeling has been performed for sensitivity and fragility analysis with the goal of providing usable input for the development of fragility curves to the *OpenSRA*.

Conclusions

Regarding direct shear displacement across wells:

- Displacement on a fault that intersects wells could occur at any depth, but wells are most vulnerable to fault displacements at shallow depths, where the gas pressure in the well is higher than the surrounding formation and gas could leak.
- Fault geometry, such as fault angle relative to the well and the fault width, are the most significant parameters that influence casing and tubing strains for a given fault shear displacement. Other parameters such as cement properties can also be significant depending on the well design.
- Details of the well design, such as the relative radii of tubing and casing and the presence of cement can have a significant impact on shear-induced casing and tubing strains. In particular, uncemented wells are able to resist greater fault displacements than cemented wells.

Regarding seismic ground shaking impact on wells:

- Ground motion from a seismic event induces the largest impact in terms of bending moment in well casings and tubing at a depth of a few meters below the ground surface.
- The height and mass of the wellhead and the soil shear strength are the most significant parameters influencing the bending moments for a given PGA in the seismic wave train.

Regarding potential caprock leakage:

- Upward gas leakage from the gas reservoir would require a gas reservoir pressure higher than the water pressures in the overlying formations, which are usually the hydrostatic water pressures.
- In the case of reservoir pressure higher than the overlying water pressure, upward gas release may occur, but it would require a substantial increase in fluid transmissivity along a fault crossing the caprock.
- The fluid transmissivity of a fault, and in particular its change with fault slip, are difficult parameters to estimate, but may be bounded within relatively broad limits based on field observations and empirical fault scaling relations.

Implementation into OpenSRA

In each of the three subtasks, advanced full-physics modeling was performed for sensitivity and fragility analyses, which were then used to develop fragility curves for the *OpenSRA* risk assessment tool. Relevant damage measures were selected as; (1) plastic strain in casing and tubing for direct fault shear across wells, (2) maximum bending moment for ground motion impact on wells, and (3) cumulative gas leakage amount for potential caprock leakage. The variability of those damage measures for a given fault shear displacement or for a given seismic time series was evaluated by varying the parameters found in the sensitivity analyses to be the most important. Finally, several second order multivariate polynomial functions were fitted to the simulation results to approximate the relationship between the damage measure (plastic strain, maximum bending moment, and cumulative leakage amount) and the intensity measure [Peak Ground Acceleration (PGA)] along with the key model parameters identified by the sensitivity analysis studies. These provide the fragility functions, i.e. probability of failure as a function of shear displacement or PGA that are implemented into *OpenSRA*. The fragility functions will be further explored and presented in the System Wide Natural Gas Infrastructure Response and Fragility Model Report, which will be published later this year.

Recommendations for Future Research

The work presented in this report can be regarded as a framework and demonstration for compiling and analyzing inputs used to improve fragility functions related to the subsurface component of an underground gas storage infrastructure. The calculated variability of the damage measures, i.e., plastic strains and bending moments in well casing and tubing and in leakage rates through activated faults, will be used to derive fragility functions for *OpenSRA*.

Recommended future work includes:

1. Expanded analysis of the fault displacement impact on the shallowest parts of wells, e.g., surface casings, and for other modes of fault activation, such as oblique slip.
2. Expanded analysis of the ground shaking impact on wells that implements a fully nonlinear elastoplastic approach to the soil column response. The equivalent-linear method used in this work may not be suitable for larger ground motions, as deamplification as a function of depth is likely overestimated (Mir Mohammad Hosseini et al., 2012). Also, it may be worth improving on the modeling of vertical ground motions as the approach applied here may also only be appropriate for weak ground motions (Tsai et al., 2017). However, the maximum bending moment recorded along

the casing system appears to be less sensitive to the vertical ground motions than to the horizontal ground motions.

3. Regarding fault slip-induced caprock leakage, the impact of water flow into a gas reservoir could be analyzed in addition to gas leakage out of the reservoir. Further research is needed to understand how fluid transmissivity along faults changes with fault activation, and how this may vary from one site to another depending on the local host rock properties.

GLOSSARY AND LIST OF ACRONYMS

Term	Definition
API	American Petroleum Institute
CalGEM	California Geologic Energy Management Division
CCST	California Council of Science and Technology
Fiber section	OpenSees object with a general geometric configuration formed by subregions of simpler and regular shapes called patches (e.g., quadrilateral, triangular or circular).
Fragility	Probability of failure
LBNL	Lawrence Berkeley National Laboratory
LCI	Lettis Consultants International
LOC	Loss of Containment
OpenSRA	Open-Source Seismic Risk Assessment
PEER	Pacific Earthquake Engineering Research Center
TAC	Technical Advisory Committee
TOUGH	Transport Of Unsaturated Groundwater and Heat
UGS	Underground Gas Storage

REFERENCES

API (2018). API Specification 5CT, 10th Edition. American Petroleum Institute. Washington, DC. https://www.api.org/products-and-services/standards/important-standards-announcements/standard-5ct.

Caine J.S., Evans J.P., Forster C.B. (1996). Fault zone architecture and permeability structure. Geology 24 (11), 1025–1028. November 1996. https://doi.org/10.1130/0091 7613(1996)024%3C1025:FZAAPS%3E2.3.CO;2.

CCST (2018). Long Term Viability of Underground Natural Gas Storage in California, An Independent Review of Scientific and Technical Information. California Council on Science and Technology, Sacramento, CA. http://ccst.us/projects/natural_gas_storage/publications.php.

Cornell, C.A. (1968). Engineering seismic risk analysis. Bull. Seismo. Soc. Am., V58(5), 1583-1606, doi: 10.1785/BSSA0580051583.

Davis, T.L., Namson, J.S., & Gordon S. (2015). Ventura basin oil fields: Structural setting and petroleum system, field trip #5, May 7, 2015. Joint annual meeting of PSAAPG and Coast Geological Society, May 2-8, 2015. 58 pp.

Dusseault, M., Bruno, M., & Barrera, J. (2001). Casing shear: Causes, cases and cures. SPE Drill. & Compl., 16 (02): 98–107. Paper Number: SPE-72060-PA. https://doi.org/10.2118/72060-PA.

Evans, D.J. (2009). A review of underground fuel storage events and putting risk into perspective with other areas of the energy supply chain, in Underground Gas Storage, Worldwide Experiences and Future Development in the UK and Europe, The Geological Society, London, Special Publications, 313, pp.173–216.

Evans, D.J., & Schultz, R.A. (2017). Analysis of occurrences at underground fuel storage facilities and assessment of the main mechanisms leading to loss of storage integrity, American Rock Mechanics Association, ARMA, 17-265, 27 pp.

Ganpatye, A., & Ramamoorthy, S. (2019). Wellbore loading assessment Aliso Canyon Gas Storage Field. Draft report to Morgan, Lewis & Bockius LLP prepared by Stress Engineering Services Inc., Houston, TX, 296p.

Folga, S., Portante, E., Shamsuddin, S., Tompkins, A., Talaber, L., McLamore, M., Kavicky, J., Conzelmann, G & Levin, T. (2016). U.S. Natural Gas Storage Risk-Based Ranking Methodology and Results. Report ANL-16/19, Argonne National Laboratory, 122pp.

Fredrich, J.T., Argüello, J.G., Deitrick, G.L., & DeRouffignac, E.P. (2000). Geomechanical modeling of reservoir compaction, surface subsidence and casing damage at the Belridge Diatomite field. SPE Reservoir Eval. & Eng. 3(4) 348–359 (SPE 65354).

Guo, B. & A. Ghalambor (2005). Natural gas engineering handbook. Gulf Publishing Company, Houston, Texas.

Hough, S.E. & Bilham, R. (2018). Revisiting earthquakes in the Los Angeles, California, basin during the early instrumental period: Evidence for an association with oil production. Journal of Geophysical Research: Solid Earth, 123, 10684-10705. https://doi.org/10.1029/2017JB014616.

Hughes, J.P., Won, W., & Erickson, R.C. (1990). Earthquake damage to the Coaling Oilfields. In the Coalinga, California, earthquake of May 2. 1983. US Geological Survey Professional Paper 1487, 399–408.

Idriss, I.M., & Seed H.B. (1970). Soil Moduli and Damping Factors for Dynamic Response Analysis. Earthquake Engineering Research Center, Report No. EERC70-10, University of California, Berkeley, 48p.

Idriss, I. M., & Seed, H.B. (1968). Seismic response of horizontal soil layers. Journal of the Soil Mechanics and Foundations Division, 94(4), 1003–1031. doi: 10.1061/JSFEAQ.0001163.

Idriss, I.M, & Sun, J. I. (1993). User's manual for SHAKE91: A computer program for conducting equivalent linear seismic response analyses of horizontally layered soil deposits. Center for Geotechnical Modeling, University of California, Davis.

Itasca Consulting Group (2020). FLAC3D — Fast Lagrangian Analysis of Continua in Three-Dimensions, Ver. 7.0. https://www.itascacg.com/software/FLAC3D.

Hashash, Y., Groholski, D., Phillips, C., Park, D., & Musgrove, M. (2011). DEEPSOIL 5.0, user Manual and Tutorial. University of Illinois, Urbana, IL, USA.

Kottke, A. R., & Rathje, E. M. (2009). Technical manual for Strata. PEER Report 2008/10. Pacific Earthquake Engineering Research Center, College of Engineering, University of California, Berkeley, CA.

Kramer, Steven Lawrence. (1996). *Geotechnical Earthquake Engineering*. Prentice-Hall, Upper Saddle River, NJ, 653 pp.

Luu, K., Jordan, P., Foxall, W., Rutqvist J. (2022). Dynamic seismic analysis of wellbore integrity. A Report for the "Performance-based Earthquake Engineering Assessment Tool for Natural Gas Storage and Pipeline Systems" Project. PEER Report 2022/##, Pacific Earthquake Engineering Research Center, University of California, Berkeley, CA.

McKenna, F. (2011). OpenSees: A framework for earthquake engineering simulation. Computing in Science & Engineering 13(4):58–66. doi: 10.1109/MCSE.2011.66.

Mir Mohammad Hosseini, S. Majdeddin, and Mojdeh Asadollahi Pajouh. 2012. "Comparative Study on the Equivalent Linear and the Fully Nonlinear Site Response Analysis Approaches." Arabian Journal of Geosciences 5(4):587–97. doi: 10.1007/s12517-010-0228-9.

Pruess, K., C. Oldenburg, and G. Moridis (2011). TOUGH2 User's Guide, Version 2. LBNL-43134. Lawrence Berkeley National Laboratory, CA.

Salem, A.C., Naruk, S.J., & Solum J.G. (2022). Impact of natural fractures on production from an unconventional shale: The Delaware Basin Wolfcamp shale. AAPG Bulletin, v. 106, no. 1 (January 2022), pp. 1–20. DOI:10.1306/07272118227.

Sasaki, T., Jordan, P., Foxall, W., & Rutqvist J. (2022). Fragility of Wells due to Fault Shearing—The Impact of Fault Displacement on the Integrity of Natural Gas Storage Wells in California. A Report for the "Performance-based Earthquake Engineering Assessment Tool for Natural Gas Storage and Pipeline Systems" Project. PEER Report 2022/##, Pacific Earthquake Engineering Research Center, University of California, Berkeley, CA.

Schnabel, P.B., Lysmer, J., & Seed, H.B., (1972). SHAKE: a computer program for earthquake response analysis of horizontally layered sites. Report No. EERC72-12, University of California, Berkeley, 88p.

Scott, Michael H. (2011). Numerical Integration Options for the Force-Based Beam-Column Element in OpenSees. Force-Based Element Integration Options in OpenSees 1–7. School of Civil and Construction Engineering, Oregon State University, Corvallis, OR.

Torabi, A. & Berg S.S. (2011). Scaling of fault attributes: A review. Marine and Petroleum Geology 28, 1444e1460.

Tsai, Chi-Chin, & Hsing-Wen Liu. (2017). "Site Response Analysis of Vertical Ground Motion in Consideration of Soil Nonlinearity." Soil Dynamics and Earthquake Engineering 102:124–36. doi: 10.1016/j.soildyn.2017.08.024.

Wells, D.L., & Coopersmith, K.J. (1994). New empirical relationships among magnitude,rupture length, rupture width, rupture area, and surface displacement. Bulletin of the Seismological Society of America 84 (4), 974e1002.

Wibberley, C.A.J., & Shimamoto, T. (2003). Internal structure and permeability of major strike-slip fault zones: the Median Tectonic Line in Mie Prefecture, Southwest Japan. Journal of Structural Geology 25 (1), 59e78.

Yang, S.-Q., Yin, P.-F., & Xu, S.-B. (2021). Permeability Evolution Characteristics of Intact and Fractured Shale Specimens. Rock Mechanics and Rock Engineering (2021) 54:6057–6076. https://doi.org/10.1007/s00603-021-02603-y.

Zhang, Y., Jordan, P., Foxall, W., Rutqvist J. (2022). Fragility Analysis Related to Caprock Leakage from Underground Gas Storage Reservoirs. A Report for the "Performance-based Earthquake Engineering Assessment Tool for Natural Gas Storage and Pipeline Systems" Project. PEER Report 2022/##, Pacific Earthquake Engineering Research Center, University of California, Berkeley, CA.

Zhu, M., McKenna, F., & Scott M.H. (2018). "OpenSeesPy: Python Library for the OpenSees Finite Element Framework." SoftwareX 7:6–11. https://doi:10.1016/j.softx.2017.10.009.

Zoback, M.D., & Gorelick S.M. (2012). Earthquake triggering and large-scale geologic storage of carbon dioxide, Proceedings of the National Academy of Sciences, 2012, 109: 10164–101168.